Characteristic analysis and suppression strategy of the valve impulse exhaust noise

A dissertation submitted to

The University of Tokushima

for the degree of

Doctor of Engineering Science

By

Jingxiang Li

The University of Tokushima

June, 2013

Abstract

for thesis entitled

Characteristic analysis and suppression strategy of the valve impulse exhaust noise

submitted by

Jingxiang Li

for the degree of Doctor of Philosophy

at the University of Tokushima

in July 2013

Pneumatic systems widely exist in the industrial productions, using high pressure compressed air as power source. The air charging and discharging processes of pneumatic cylinder through valves are recurrent to generate aerodynamic noise, especially the venting exhaust to atmosphere directly. In order to suppress this kind of impulse exhaust noise, the characteristics of such noise and the suppression strategy are presented. The aerodynamic properties of impulse exhaust are studied firstly. Based on the analysis of aerodynamic parameters during the exhaust process, the sound sources are discussed. Then the radiated noise of exhaust with a typical sintered bronze silencer is predicted both in time-domain and frequency-domain. A noise suppression strategy of controlling the opening process of valve is proposed. Finally the experiments based on a modeled

pneumatic exhaust system and a pneumatic friction clutch and brake system of mechanical press are carried out to verify the validity of the presented model and the suppression strategy.

In Chapter 1, the impulse exhaust noise will be introduced briefly, including the definition, characteristics and harm to the environment. Then the research background of pneumatic exhaust, the progress of classical exhaust noise control and the purpose of this study will also be introduced.

In Chapter 2, analysis of aerodynamic properties of impulse exhaust will be presented in details. The typical pneumatic exhaust systems will be introduced firstly. Then based on some basic assumptions, the mathematic model of aerodynamic properties of pneumatic exhaust will be described. A one-dimensional thermodynamic model is used to describe the transient exhaust process. So the aerodynamic parameters during the exhaust can be obtained, such as cylinder pressure, mass flow rate. In addition, the movement equation of piston in the cylinder of typical pneumatic friction clutch and brake system will be introduced to describe the whole systems. In practice, some classical porous materials are used to reduce the impulse noise. The aerodynamic model of porous material with rigid frame, such as sintered bronze used in muffler devices normally, will also be obtained.

In Chapter 3, the sound sources of impulse exhaust noise will be introduced according to the Lighthill's general theory, as the impulse exhaust noise is a kind of aerodynamic noise. The impulse exhaust noise is mainly composed of monopole sources related to the mass flow and quadrupole sources generated by the turbulence. Based on a piston sound source assumption, the noise radiation characteristics of the exhaust with sintered bronze muffler will be predicted. The mass flow considered as a monopole source is related to the sound pressure of impulse exhaust noise. And the sound pressure level (SPL) at a far-field observation point is predicted by the piston acoustic source

approximation.

In Chapter 4, the control strategies of impulse exhaust noise will be presented. There are three approaches to control the noise from the sound source, the propagation path and the receiver, respectively. Muffler devices are used to reduce the aerodynamic jet noise classically. The features and disadvantages of various mufflers in the industrial applications will be introduced firstly. Unlike the steady noise or period noise, the evaluations of impulse noise are introduced. Then a semi-active control strategy to change the sound source of impulse exhaust by controlling the opening process of exhaust valve is presented. The principle and specific control method will be introduced.

In Chapter 5, experimental study will be presented. The experiments were based on a pneumatic friction clutch and brake (PFC/B) system of mechanical press and also a simplified cylinder exhaust system. In order to test the presented semi-active noise control strategy, a modified pneumatic valve was designed, which can adjust the poppet valve by a servo motor. The experimental results will be shown to verify the validity of the presented aerodynamic model and the radiated noise predictions. The noise was analyzed to study the effect of presented suppression strategy comparing to the direct exhaust.

In conclusion, the aerodynamic properties of impulse exhaust based on typical pneumatic exhaust systems have been investigated. According to the aerodynamic models, the flow parameters during the impulse exhaust were obtained. The sound sources of impulse exhaust noise were studied based on the Lighthill's general theory of aerodynamic noise. The radiated noise of exhaust with a typical sintered bronze silencer is predicted both in time-domain and in frequency-domain. In addition, a semi-active noise control strategy has been presented to suppress the impulse exhaust noise especially to reduce the peak SPL.

CONTENTS

Chapter 1 Introduction

Pneumatic systems widely exist in the industrial productions, using high pressure compressed air as power source. The air charging and discharging processes of pneumatic cylinder through valves are recurrent to generate aerodynamic noise, especially the venting exhaust to atmosphere directly[1-5]. The transient exhaust is choked and sonic at the valve throat since the high pressure of compressed air larger than 0.3 MPa normally[6-8]. During the exhaust process, the potential energy of compressed air in the cylinder is converted to kinetic energy while the air flow is accelerated through the valve generating the impulse exhaust noise with short duration. The sound pressure of impulse exhaust noise is changed acutely because of the rapid flow change via the valve. It will cause serious environment pollution and hearing damages for workers due to the large sound pressure of exhaust noise with the peak value normally more than 130 dB. Thus, several researches both on the mechanism and reduction methods of air exhaust noise were studied in recent years[9-12].

1.1 Properties of impulse exhaust noise

As indicated in the previous statement, the impulse exhaust noise is a kind of aerodynamic noise generated by the unsteady jet. According to the noise fluctuation value, exhaust noise is divided into steady exhaust noise, periodical exhaust noise and intermittent or impulse exhaust noise. As a special jet noise, the impulse exhaust noise is also caused by high-velocity jets and the turbulent eddies generated by shearing flow. Such noise is known as broadband noise and extends well beyond the range of human hearing. The sound generated by high-speed jets is usually

associated with several different he sound generated by high-speed jets is usually associated with several different sources acting simultaneously, such as jet mixing noise caused by the turbulent mixing of the jet with the ambient medium, and shock-associated noise for imperfectly expanded supersonic jets produced by the convection of turbulence through shock cells in the jet[1,13]. Different from the normal steady jet noise and periodical jet noise, the impulse exhaust noise has a significant impulse property.

1.1.1 Brief description of impulse exhaust noise

Impulse noise was first introduced by Rosenblith and Stevens[14]. From the results of theoretical and experimental investigations, they argued that some judgment is required to distinguish between impulse and continuous noise[15,16]. Figure 1 schematically types the pressure-time histories of these noises. Steady noise has a nearly constant pressure level at a measuring point with no or only extremely small fluctuations. Unsteady noise has irregular and continuous signals over a wide range of sampling period. Of the signals that intermittently arise at a time interval, intermittent noise has the duration time of each pulse signal over several seconds. The intervals between the pulse signals may be nearly constant or irregular. The definition of impulse noise varies from country to country and there is still no consistent definition. A recommendation from the International Standard Organization ISO2204 stated that an impulse noise can be characterized as a burst sound or continuous burst sounds with a duration time less than one second[17]. This indicates that if an impulse noise is produced within the time interval mentioned above, an adjustment should be necessary to find the equivalent sound pressure level. On the other hand, IEC argued that an impulse noise can be a single-pulse sound or a burst sound with a duration

time between 0.001 and 1 s[18]. Anyway, the exhaust noise studied in this paper belongs to impulse noise.

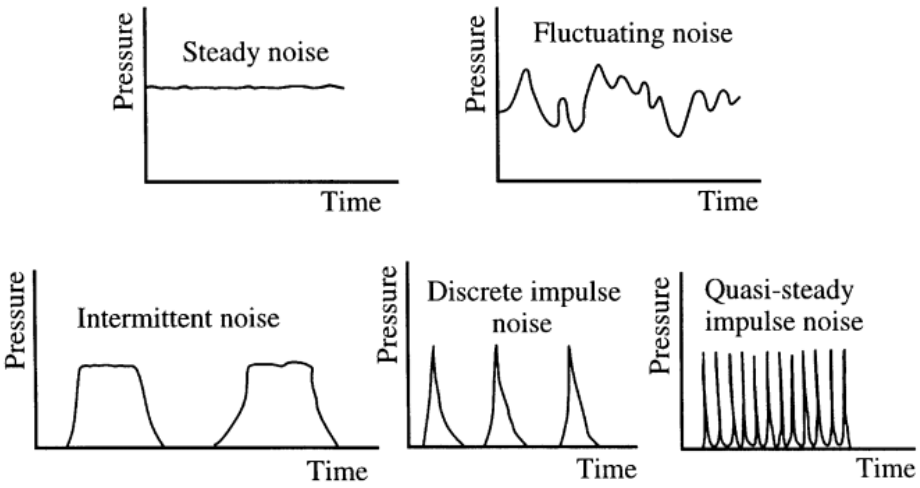

Figure 1-1[19] Classification of noises based on the pressure-time histories.

In this paper, impulse noise is defined as a short-duration sound characterized by a shock front pressure waveform (i.e. virtually instantaneous rise), usually created by a sudden release of energy; for example, as encountered with explosives or gun blasts[1]. Such a characteristic impulse pressure waveform is often referred to as a Friedlander wave, and is illustrated in Figure 1-2(a). This single impulse waveform is typically generated in free-field environments, where sound reflecting surfaces that create reverberation are absent. With gunfire, mechanically generated noise is also present in addition to the shock pulse, and in this case the waveform envelope can take the form illustrated in Figure 1-2(b).

The durations of impulsive noises may vary from microseconds up to 50 ms, although in confined spaces reverberation characteristics may cause the duration to extend considerably longer. In all cases, however, the characteristic shock front is present. For the purpose of assessing hearing damage risk, a duration time has been defined as the time required for the peak level to drop 20 dB, as illustrated in Figure 1-2.

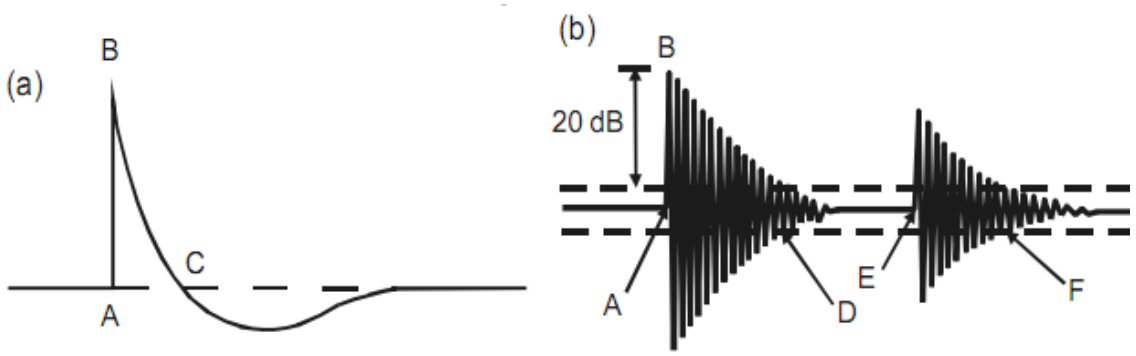

Figure 1-2[1] Idealized waveforms of impulse noise. Peak level is the pressure difference AB; duration time is the time difference AD (+EF when a reflection is present).

Pneumatic devices quite often eject gas (air) in the form of high-pressure jets. Such jets can be very significant generators of noise. Different from the combustion engine exhausts, there are many kinds of exhaust is a transient process, such as the exhaust of pneumatic friction clutch and brake (PFC/B) cylinders. In the practical work, the exhaust process is very short to ensure the coordination of the PFC and PFB. Furthermore, such kind of pneumatic exhaust has characteristics of high-pressure exhaust (pressure ratio normally more than 3) and large gas displacement. Thus, it will generate huge impulse noise of as high as 125 dB(A), with the peak sound pressure more than 130 dB(A) [3].

1.1.2 Harm of impulse exhaust noise

Industrial noise is usually considered mainly from the point of view of environmental health and safety, rather than nuisance, as sustained exposure can cause permanent hearing damage[1,13,20]. Exposure to excessive noise for a short period of time may produce a temporary loss of hearing sensitivity. If this happens, the subject may notice a slight dulling in hearing at the end of the exposure. This effect is often accompanied by a ringing in the ears, known as tinnitus,

which persists after the noise exposure. This temporary loss of hearing sensitivity is known as temporary threshold shift (TTS) or auditory fatigue. Removal from the noise generally leads to more or less complete recovery if the exposure has not been too severe. If the noise exposure is severe or is repeated sufficiently often before recovery from the temporary effect is complete, a permanent noise-induced hearing loss may result.

The elevated sound levels cause trauma to cochlear structure in the inner ear, which gives rise to irreversible hearing loss. A very loud sound in a particular frequency range can damage the cochlea's hair cells that respond to that range, thereby reducing the ear's ability to hear those frequencies in the future; however, loud noise in any frequency range has deleterious effects across the entire range of human hearing. The outer ear (visible portion of the human ear) combined with the middle ear amplifies sound levels by a factor of 20 when sound reaches the inner ear.

Noise can not only cause hearing impairment (at long-term exposures of over 85 dB(A), known as an exposure action value), but it also acts as a causal factor for stress and raises systolic blood pressure. Additionally, it can be a causal factor in work accidents, both by masking hazards and warning signals, and by impeding concentration.

In general, people are not habitually exposed to impulsive noises. In fact, only people exposed to explosions such as quarry blasting or gunfire are exposed to impulse noises. Estimates of the number of pulses likely to be received on any one occasion vary between 10 and 100, although up to 1000 impulses may sometimes be encountered.

The noise level below which damage to hearing from habitual exposure to noise should not occur in a specified proportion of normal ears is known as the hearing damage risk criterion. Internationally, the hearing damage risk criterion has been set at 90 dB(A) for a continuous

eight-hour exposure each day to ordinary broadband noise. Moreover a criterion of 85 dB(A) for an eight-hour daily exposure is encouraged to minimize the hearing loss in some criterions. To the impulse noise, the criterion is related to the exposure impulse numbers every day. The acceptable numbers of impulse noise of 140 dB and 130 dB are 100 and 1000, respectively[3].

1.2 Research background

As the previous statements, the impulse exhaust noise has a serious pollution to the environment and harm to people. In this section, the common pneumatic systems generating the exhaust noise would be introduced. The mechanism study of impulse exhaust noise would be presented. It would be also presented the outstanding studies on the exhaust noise control.

1.2.1 Pneumatic systems

The pneumatic systems such as PFC/B systems and pneumatic clamps shown in figure 1-3 are widely exist in the industrial applications. The intake and exhaust processes are controlled by a pneumatic directional valve. When the high pressure air is supplied into the PFC cylinder, the piston will be pushed to joint the friction disk so that the slider-crank mechanism will be driven by the main motor. When the valve is switched to vented the air inside the cylinder, the piston will be returned by the returning spring and unclench the friction disk. In the practical work, the air pressure supplied into the cylinder normally more than 0.5 MPa, so the sonic choked exhaust will happens during the exhaust process. As same as the PFC/B systems, the pneumatic clamp works by injecting and exhausting the air of cylinder alternately, so that the work piece could be clamped and unclenched. In the production process, workers are normally beside the equipment or devices, thus

the huge impulse exhaust noise will bring harm to them as indicated in previous.

(a) (b)

Figure 1-3 Pneumatic systems. (a) PFC of a mechanical press; (b) pneumatic clamp.

1.2.2 Mechanism study of impulse exhaust noise

The aerodynamic noise is one of the most important environment pollution sources. Lighthill's general theory has played a leading role to the studies on the mechanism of aerodynamic noise[21-25]. Considering the mass flow source Q, the body force F_i on the fluid and the source caused by the fluctuations, the wave equation of sound has the expression as:

$$\frac{\partial^2 \rho}{\partial t^2} - c^2 \nabla^2 \rho = \frac{\partial Q}{\partial t} - \frac{\partial F_i}{\partial x_i} + \frac{\partial^2 T_{ij}}{\partial x_i \partial x_j}, \tag{1-1}$$

where T_{ij} is the Lighthill's stress tensor.

The sound sources of aerodynamic noise are divided into three types as monopole source, dipole source and quadrupole source. The characteristics of sound sources including source behavior, directivity, sound power and acoustic efficiency are list in Table 1-1. The monopole sound

source is related to the mass flow rate at the exhaust outlet. The sound power of monopole is

$$W_{\mathrm{m}} \propto \rho^2 v^4 D^2 / (\rho_0 c_0) = \rho^2 v^3 D^2 M / \rho_0 . \tag{1-2}$$

where v is the exhaust velocity, D is the diameter of outlet, ρ and c are the density and sound speed of exhaust air, ρ_0 and c_0 are the density and sound speed of surrounding air, M is the Mach number.

The dipole sound source is related to the force of flow and solid body. It can be seen as composed by two monopoles. The sound power of dipole source is the form as:

$$W_{\mathrm{d}} \propto \rho^2 v^6 D^2 / (\rho_0 c_0^3) = \rho^2 v^3 D^2 M^3 / \rho_0 . \tag{1-3}$$

When the flow velocity is very high, the Lighthill's stress tensor T_{ij} is changed in the flow field to generate quadrupole sound source. It can be seen as a pair of 180° phase dipoles. The radiated sound power is the expression as:

$$W_{\mathrm{q}} \propto \rho^2 v^8 D^2 / (\rho_0 c_0^5) = \rho^2 v^3 D^2 M^5 / \rho_0 . \tag{1-4}$$

Table 1-1 Three types of basic sound sources

Source type	Source behavior 180° phase difference	Directivity	Sound power ratio	Acoustic efficiency ratio
Monopole			$\rho^2 v^4 D^2 / (\rho_0 c_0) = \rho^2 v^3 D^2 M / \rho_0$	M
Dipole	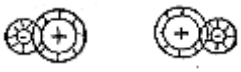		$\rho^2 v^6 D^2 / (\rho_0 c_0^3) = \rho^2 v^3 D^2 M^3 / \rho_0$	M^3
Quadrupole	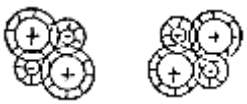		$\rho^2 v^8 D^2 / (\rho_0 c_0^5) = \rho^2 v^3 D^2 M^5 / \rho_0$	M^5

In the exhaust process of PFC/B systems, the transient exhaust is choked and sonic exhaust occurs at the throat (Mach number equals to 1) most of the time since the initial pressure in cylinder is usually more than 0.3 Mpa [26-30]. Maa [6] indicated that as the pressure ratio between 3 to 5 particularly, the noise generated by transient exhaust is entirely dominated by impulsive noise. The noise always more than 120 dB mainly contains in high-frequency because of the impulse characteristic [7-9]. Sintered bronze silencer is always used to suppress this kind of exhaust noise. Besides reducing the noise, the aerodynamic property of silencer is also an important factor of the equipment for the normal and safe operation [7]. The descriptions of pressure drop in the porous materials have been studied for decades. Ergun equation, one of the descriptions, was first given by Ergun [31] and then verified and developed by many later workers [32-35]. For high velocity flow, both the viscous energy loss, proportional to the superficial velocity and the correction for inertial losses in the porous medium are considered. It originally describes the relationship between the pressure drop and the parameters of porous medium composed of spherical particles such as porosity and particle diameter.

According to Lighthill sound analogy [21,22], the transient exhaust noise is mainly composed of monopole sources related to the mass flow and quadrupole sources generated by the turbulence [9,28]. Therefore the flow generated noise is closely related to the aerodynamic parameters of the transient exhaust. Zhao et al. [9] applied the Lighthill's aerodynamic noise generated theory to predict the intermittent exhaust noise with expansion chamber muffler, and the results were close to the experiments at high-frequency. Shi [7] furthermore considered the transient flow at the outlet of ducts as an approximating piston acoustic source and analyzed the octave spectrum of the exhaust noise without silencers, of which the errors were less than 3.5 dB from 250 Hz to 16 kHz. The

acoustic propagation and absorption properties of porous materials are described first by Kirchhoff with a phenomenological model of viscous and thermal effects created in cylindrical tubes with circular cross-section [36]. In addition, the macroscopic description by two parameters, namely, the effective density and bulk modulus (or compressibility) is used to predict the sound absorbing performance of porous materials with complex geometry. Johnson-Champoux-Allard model, the widely accepted and used theoretical model, presents a description assuming the porous layer as an equivalent fluid. The formulation of effective density is proposed by Johnson et al. [37] and improved by Pride et al. [38] to express the dynamic viscous permeability. Similar descriptions of thermal exchanges related to Bulk modulus is modeled by Champoux and Allard [39] and Lafarge et al. [40] later. Based on the equivalent models, the classical transfer matrix method (TMM) is often used to obtain the acoustic properties of a certain porous material or multilayer materials conveniently and rapidly [41-43]. Moreover, impulsive excitations generated the discharge from a high pressure air tank were used for the prediction of acoustic response of absorbent material using the characteristic impedance and wavenumber [44-46].

1.2.3 Progress of exhaust noise control

Until now, reduction of impulse noise due to pneumatic exhaust has largely been achieved by passive devices. Muffling devices or silencers are commonly used to reduce noise associated with internal combustion engine exhausts, high pressure gas or steam vents, compressors and fans. These examples lead to the conclusion that a muffling device allows the passage of fluid while at the same time restricting the free passage of sound. Muffling devices may function in any one or any combination of three ways: they may suppress the generation of noise; they may attenuate noise

already generated; and they may carry or redirect noise away from sensitive areas.

Since 1950s, the reactive mufflers were studied to reduce the noise in industrial. The expansion chamber and side branch resonator were used in the exhaust noise suppression. Four terminal parameter method evolved from the equivalent circuit improved the study of acoustic characteristics of the reactive devices[47-49]. Furthermore, many works also researched the properties of such reactive devices with flow. However, these studies were almost based on the noise control with steady flow conditions. Later, finite element method (FEM) and boundary element method (BEM) were used to simulate the sound field inside the mufflers, and obtain the properties such as transmission loss.

The investigation of active noise control theory was developed and studied by many workers since 1960s. This method has a significant suppression on the one-dimensional noise of specific frequency such as noise generated by steady flow; but is difficult to reduce the high-frequency noise[50,51].

In order to reduce the pneumatic exhaust noise, various mufflers were designed as shown in Figure 1-4[12,52-56]. Expansion chamber mufflers as the simplest reactive muffler suddenly expand and reduce the cross-section area to reflect the sound wave back to the source and reduce the amount of acoustic energy transmitted. They have good performance at low frequencies and are useful in harsh environments. Unlike reactive mufflers, absorptive mufflers which incorporate sound absorbing porous materials such as fiberglass, mineral wool and high-porosity foams to transform acoustic energy into heat. Absorbing materials have some disadvantages including pollution, the risk of high heat and limited lifetime therefore they may become ineffective and impractical. Nevertheless, the porous mufflers are widely used in the pneumatic exhaust noise

reduction because of the desirable characteristics for broadband noise. Perforated panel with wide absorption sound spectrum and high sound absorption coefficient was studied and applied to suppress the industrial noise in recent decades. The low back pressure characteristic of perforated panel ensures the air being expelled smoothly. In the application of IEN control, the noise reduction, the flow resistance and the structure cost should be all considered as the evaluations of muffler.

(a) (b)

(c) (d) (e)

Figure 1-4[12] Various muffler devices. (a) Expansion chamber muffler; (b) perforated panel muffler; (c) Foam plastic muffler; (d) Polyethylene resin muffler; (e) sintered bronze muffler.

1.3 Thesis organization

In this dissertation, the aerodynamic properties and radiated noise characteristics of impulse exhaust would be studied. The aerodynamic model of impulse exhaust was presented. The sound

sources of impulse exhaust noise and the radiated noise prediction was also introduced. Then a semi-active noise control strategy was proposed to suppress the peak SPL of impulse exhaust noise. The experiments were carried out to verify the presented models and noise control strategy.

1.3.1 Scope

1. Modeling the impulse exhaust process as an initial value problem for ordinary differential equations.
2. Investigate the aerodynamic properties of porous material with rigid frame such as sintered bronze material by Ergun equation.
3. Predict the radiated noise generated by exhaust with a sintered bronze silencer according to a piston sound source approximation.
4. A semi-active noise control strategy by controlling the opening process of valve was investigated. In order to verify the strategy, a modified valve driven by a servo motor was designed and tested in a pneumatic cylinder exhaust system.

1.3.2 Signification

1. The mathematic model of aerodynamic properties of impulse exhaust based on thermodynamics can be solved conveniently. Combing the model of porous material with rigid frame, it can help to analyze and improve the aerodynamic properties of various silencers.
2. According to the presented radiated noise characteristics and piston sound source approximation, the radiated exhaust noise at far field can be predict both in time-domain and

in spectrum.

3. The effect of effective cross-sectional area of valve on the impulse exhaust noise was investigated. According to the proposed noise control strategy, the sound source of impulse exhaust noise will be changed so that the noise can be suppressed especially reducing the peak SPL.

Chapter 2 Aerodynamic properties of impulse exhaust

In this chapter, analysis of aerodynamic properties of impulse exhaust will be presented in details. The typical pneumatic exhaust systems will be introduced firstly. Then based on some basic assumptions, the mathematic model of aerodynamic properties of pneumatic exhaust will be described. A one-dimensional thermodynamic model is used to describe the transient exhaust process. So the aerodynamic parameters during the exhaust can be obtained, such as cylinder pressure, mass flow rate. In addition, the movement equation of piston in the cylinder of typical pneumatic friction clutch and brake system will be introduced to describe the whole systems. In practice, some classical porous materials are used to reduce the impulse noise. The aerodynamic model of porous material with rigid frame, such as sintered bronze used in muffler devices normally, will also be obtained.

2.1 Typical pneumatic exhaust systems

Pneumatic systems are normally applied to thrust control, flow control and pressure control. Figure 2-1 shows a pneumatic exhaust system, including a cylinder, a pneumatic valve, exhaust pipes and a silencer. The cylinder in Figure 2-1 is a kind of acting cylinder, which is a typical application of pneumatic friction clutch and brake (PFC/B). It is composed of a cylinder, a piston and a returning spring. When the high pressure compressed air is supplied from compressor to the acting cylinder, the piston is pushed to the left side as the position shown in Figure 2-1 so the friction disc is engagement. Meanwhile the exhaust passage is opened, allowing the air in the cylinder to be discharged from port A to port R. The pressure in the cylinder is reduced so that the

piston will be reset by the returning spring and the friction disc will be disengagement. The high pressure air exhausts through the pipes, hybrid regulator valve and silencer to the environment immediately, and generates flow noise.

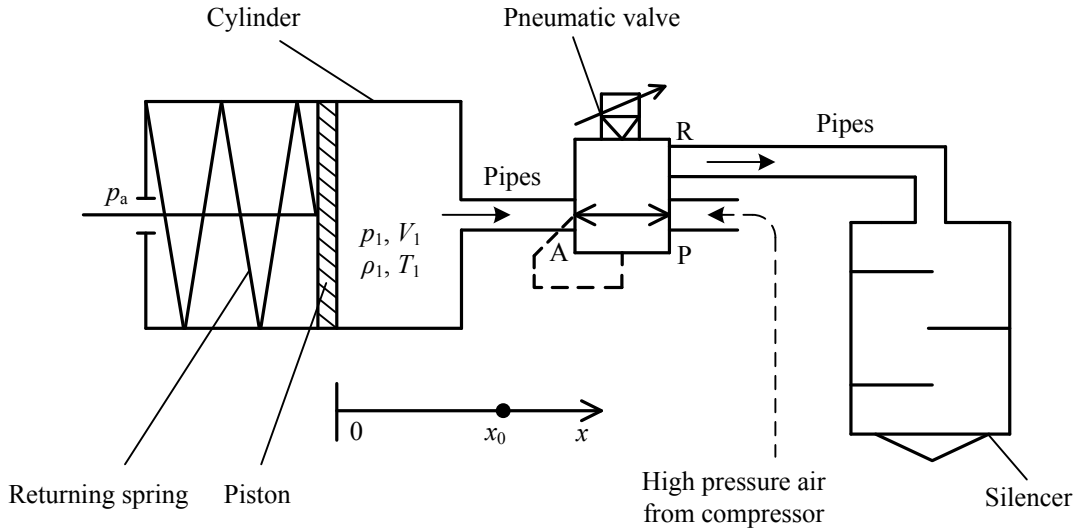

Figure 2-1 Structure of a typical pneumatic exhaust system.

The pneumatic valve used in the exhaust systems is normally a 3/2-way directional valve or a quick exhaust valve. The directional valve allows air flow into different paths from. It usually consist of a spool inside a cylinder which is mechanically or electrically controlled. The movement of the spool restricts or permits the flow, thus it controls the fluid flow. These valves make use of electromechanical solenoids for sliding of the spool. In order to facilitate the study, a hybrid regulator valve VY1700 produced by SMC Company shown in Figure 2-1 and a common 3/2 way directional valve K23J50 are used in this study. The hybrid regulator valve is created from a regulator and a solenoid valve. It is not only able to switch the flow paths, but also able to adjust the cylinder pressure by the regulator. The schematic diagram of VY1700 is shown in Figure 2-2[57]. Then the working principle of VY1700 will be introduced.

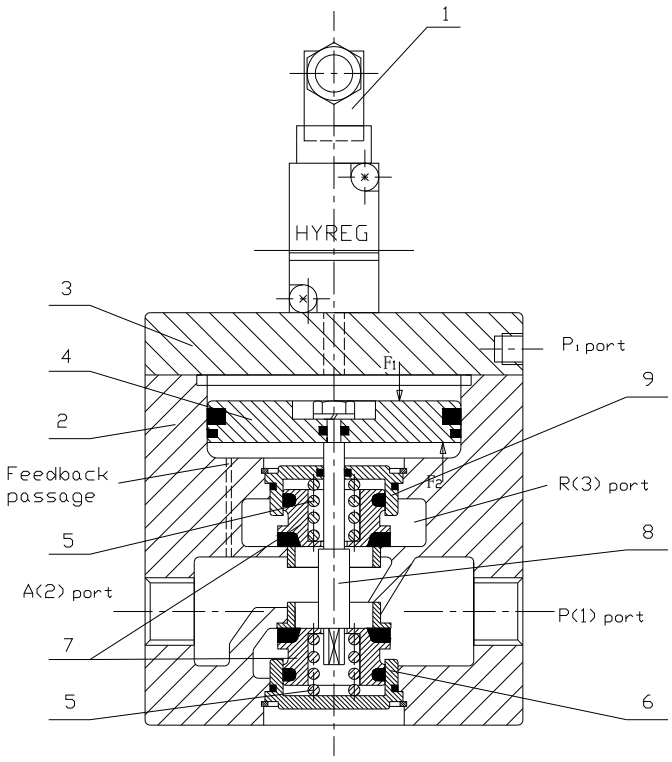

Figure 2-2 Schematic diagram of VY1700 valve. It includes 1-pilot valve, 2-body, 3-cover, 4-adjusting piston, 5-spring, 6-valve guide, 7-poppet valves, 8-shaft and 9-valve guide

The pair of poppet valves closes due to the balance between actuating forces F_1 and F_2. When the port A pressure becomes higher than the pilot pressure, F_2 becomes higher than F_1. This causes the pressure regulation piston to move upward, and the top poppet valve to open, allowing the air to be discharged from port A to port R. When the port A pressure drops to reach a balance, the regulator returns to the state shown in the Figure 2-2.

The working principle of K23J50 3/2-way directional valve is very simple. When the pilot valve is opened to supplied high pressure air into pilot cylinder, the poppet valve is pushed to move, allowing the air to be supplied from port P to port A. Conversely, when the pilot valve is closed to discharge the air in the pilot cylinder, the poppet valve is returned, closing the intake path, and allowing the air to be discharged from port A to port R.

2.2 Mathematic model description

In order to study the unsteady flow of pneumatic exhaust process, the control volume approach is introduced to establish the mathematic model. In fluid mechanics and thermodynamics, a control volume is a mathematical abstraction employed in the process of creating mathematical models of physical processes. In an inertial frame of reference, it is a volume fixed in space or moving with constant velocity through which the fluid (gas or liquid) flows. The surface enclosing the control volume is referred to as the control surface. Combining the energy equation, the mass balance equation and the characteristic equation of the gas, the parameters in the control volume can be determined while considering the exchange of heat and work done at the control surfaces.

2.2.1 Model assumptions

Considering the actual situation of pneumatic exhaust process, some assumptions are given in details in order to facilitate the study of aerodynamic characteristics[58-63].

(1) During the pneumatic exhaust process, the gas energy is instantaneously and uniformly in the total volume of cylinder. So the exhaust process is assumed to be quasi-static.

(2) The exhaust process is very short so that the exchange of heat at the walls of cylinder, pipes and valve can be neglected. The exhaust process in the pneumatic exhaust system can be approximated as an adiabatic process, and furthermore be assumed to be isentropic.

(3) Due to the cross-sectional area of cylinder is much larger than that of pipes or valve, the velocity of air in the cylinder can be ignored during the exhaust process.

(4) The air flow in the cylinder and pipes is regarded as one-dimensional flow.

(5) The air flow through the pneumatic valve can be approximated as air in the large container

or a large section of pipe flows through a convergent nozzle to the after chamber or environment, as shown in Figure 2-3.

(6) The pressure loss caused by the friction of air flow through the pipes is corrected by cross-sectional area.

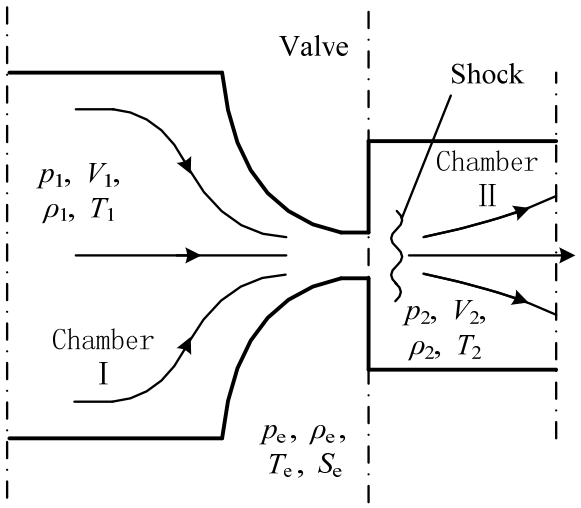

Figure 2-3 Simplified model of air flow through a pneumatic valve.

2.2.2 Thermodynamic equation of control volume

The compressed air in the system can be regarded as perfect gas. According to the first law of thermodynamics, the change in internal energy of the compressed air inside the cylinder or the muffler's chambers, of which the volume is seemed as a control-volume, is written as [64-66]:

$$\delta E = \delta Q - \delta W + h_{0\text{in}}\delta m_{\text{in}} - h_{0\text{out}}\delta m_{\text{out}}\ , \tag{2-1}$$

where E is the energy of the control-volume, and δQ and δW are the heat added to the system and the work done by the system. The last two terms of Equation (2-1) are the energy of the mass flow in and out of the control volume. Assuming the parameters in the control volume are pressure p_c, volume V_c, density ρ_c, temperature T_c, mass m_c and internal energy $e_c = RT_c/(\gamma-1)$. The

differential energy inside the control volume is expressed by:

$$\frac{\mathrm{d}E}{\mathrm{d}t}=\frac{\mathrm{d}(m_{\mathrm{c}}e_{\mathrm{c}})}{\mathrm{d}t}=\frac{1}{\gamma-1}(p_{\mathrm{c}}\frac{\mathrm{d}V_{\mathrm{c}}}{\mathrm{d}t}+V_{\mathrm{c}}\frac{\mathrm{d}p_{\mathrm{c}}}{\mathrm{d}t}), \tag{2-2}$$

according to the perfect gas equation and isentropic condition, where γ is the adiabatic coefficient of the perfect gas, R is the gas constant. Substituting the stagnation enthalpy $h_0=c_pT_0=\gamma RT_0/(\gamma-1)$, the sound velocity $c=\sqrt{\gamma RT}$ and the Equation (2-2) into the Equation (2-1), the thermodynamic differential equation in the control volume can be rewritten as:

$$V_{\mathrm{c}}\frac{\mathrm{d}p_{\mathrm{c}}}{\mathrm{d}t}+\gamma p_{\mathrm{c}}\frac{\mathrm{d}V_{\mathrm{c}}}{\mathrm{d}t}=\frac{\mathrm{d}m_{\mathrm{in}}}{\mathrm{d}t}c_{0\mathrm{in}}{}^{2}-\frac{\mathrm{d}m_{\mathrm{out}}}{\mathrm{d}t}c_{0\mathrm{out}}{}^{2}. \tag{2-3}$$

Particularly, if the volume of control volume is fixed, such as a fixed volume cylinder or the chamber of silencer, Equation (2-3) will be simplified to the following form.

$$V_{\mathrm{c}}\frac{\mathrm{d}p_{\mathrm{c}}}{\mathrm{d}t}=\frac{\mathrm{d}m_{\mathrm{in}}}{\mathrm{d}t}c_{0\mathrm{in}}{}^{2}-\frac{\mathrm{d}m_{\mathrm{out}}}{\mathrm{d}t}c_{0\mathrm{out}}{}^{2}. \tag{2-4}$$

In order to solve the state parameters of control volume during the unsteady exhaust process, the mass flow rate flow in and out of the control volume should be obtained firstly. In addition, the mass flow rate flowing out should be equal to the mass flow rate flowing in the after adjacent control volume because of the continuity of mass.

2.2.3 Mass flow rate

The air flowing through a pneumatic valve is seem as flowing through a convergent nozzle as shown in Figure 2-3. It is assumed that the stagnation parameters of air in chamber Ⅰ are p_1, ρ_1, T_1, the parameters of air in chamber Ⅱ are p_2, ρ_2, T_2, the parameters at the throat of nozzle are

p_e, ρ_e, T_e, and the effective cross-sectional area of the convergent nozzle is S_e. The quasi-static equation of the flow energy at the nozzle throat is:

$$c_1^2 = c_e^2 + \frac{\gamma - 1}{2} u_e^2 , \tag{2-5}$$

where u_e denotes the velocity of air flow through the nozzle. The mass flow rate through the convergent nozzle is $\mathrm{d}m / \mathrm{d}t = \rho_e u_e S_e$.

1) Sonic exhaust

When the pressure in chamber Ⅰ is larger than the critical value related to the pressure in chamber Ⅱ as $p_1 \geq \left[(\gamma+1)/2\right]^{\gamma/(\gamma-1)} p_2$, sonic flow happens at the throat of nozzle. The pressure at the nozzle throat is proportional to p_1 as $p_e = \left(2/(\gamma+1)\right)^{\gamma/(\gamma-1)} p_1$. The mass flow reaches maximum and the velocity of exhaust flow at the throat reaches the sound speed, so the Mach number is equal to 1. Substituting the Mach number $M_a = u_e / c_e = 1$ into Equation (2-5), the flow velocity at the throat can be obtained as:

$$u_e = \left(\frac{2}{\gamma+1}\right)^{1/2} \sqrt{\gamma R T_1} . \tag{2-6}$$

Therefore, the mass flow rate at the nozzle throat of sonic exhaust is written as:

$$\frac{\mathrm{d}m}{\mathrm{d}t} = S_e p_1 \sqrt{\frac{\gamma}{R T_1}} \left(\frac{2}{\gamma+1}\right)^{\frac{\gamma+1}{2(\gamma-1)}} . \tag{2-7}$$

2) Subsonic exhaust

When the pressure in chamber Ⅰ is smaller than the critical value related to the pressure in chamber Ⅱ as $p_1 < \left[(\gamma+1)/2\right]^{\gamma/(\gamma-1)} p_2$, subsonic flow happens at the throat of nozzle. The pressure at the nozzle throat is equal to the back pressure as $p_e = p_2$. So the flow velocity and the

mass flow rate at the throat are written as:

$$u_e = \sqrt{\frac{2\gamma RT_1}{\gamma - 1}\left(1 - \left(\frac{p_2}{p_1}\right)^{(\gamma-1)/\gamma}\right)}, \tag{2-8}$$

$$\frac{\mathrm{d}m}{\mathrm{d}t} = S_e p_1 \sqrt{\frac{2\gamma}{(\gamma-1)RT_1}\left(\left(\frac{p_2}{p_1}\right)^{2/\gamma} - \left(\frac{p_2}{p_1}\right)^{(\gamma+1)/\gamma}\right)}. \tag{2-9}$$

3) The effective cross-sectional area of valve

In the previous discussions, the effective cross-sectional area S_e of nozzle throat is a constant. However, the opening process of valve is dynamic so that S_e is a variable of time during the opening process of valve in practice. Thus, it is necessary to establish the mathematic model of variable $S_\mathrm{e}(t)$.

To the common directional valve as K23J50, when the pilot valve opens, the poppet valve is reset by the force of returning spring and cylinder air in a very short time. Assuming the displacement of poppet valve is linear in the total opening time t_0, and the maximum cross-sectional area is $S_{\mathrm{e,max}}$, the effective cross-sectional area of valve can be written as:

$$S_\mathrm{e}(t) = \begin{cases} S_{\mathrm{e,max}}\, t/t_0, & t \le t_0 \\ S_{\mathrm{e,max}}, & t > t_0 \end{cases}. \tag{2-10}$$

To the hybrid regulator valve VY1700, the effective cross-sectional area S_e is a function of the cylinder pressure or the port A pressure p and the response time t_0 of the hybrid regulator valve. Assuming that the area S_e is related linearly to the port A pressure p, the effective cross-sectional area of valve can be written as[8]:

$$S_\mathrm{e}(t) = \begin{cases} (ap - b)\, t/t_0, & t \le t_0 \\ ap - b, & t > t_0 \end{cases}, \tag{2-11}$$

where a and b are related to the parameters of returning spring, poppet valve and adjusting piston inside VY1700 valve. When the port A pressure is equal to the ambient pressure, the flow path between port A and port R is close causing by the force of returning spring.

2.2.4 Dynamic equation of piston

The exhaust process of a fixed volume cylinder through pneumatic valve can be described by the above equations. But to the acting cylinder as shown in Figure 2-1, the piston will be moved when the cylinder pressure drops. Thus, the volume of acting cylinder is variable. Neglecting the friction and viscous force, the dynamic equation of piston is

$$-k(x-x_0)+(p_{\mathrm{a}}-p_1)S=M\frac{\mathrm{d}^2x}{\mathrm{d}t^2}, \tag{2-12}$$

where x is the displacement of piston, M and S are the mass and cross-sectional area of the piston, k and x_0 are the stiffness and pre-compression length of the returning spring. Assuming the initial volume before exhaust is V_0, the variable volume will be $V_1=V_0-xS$. Therefore Equation (2-12) can be rewritten as:

$$M\frac{\mathrm{d}^2V_1}{\mathrm{d}t^2}=(p_1-p_{\mathrm{a}})S^2-k(V_1-V_0+x_0S) \tag{2-13}$$

Equation (2-12) or (2-13) is only used to describe the dynamic process of piton moving. When the cylinder pressure is large enough as $p_1>p_{\mathrm{a}}+kx_0/S$, the piston is pressed at the left limit position and the cylinder volume keeps $V_1=V_0$. Also, when the piston is reset to the right limit position x' when the solved piston displacement $x>x'$, the cylinder volume also becomes to a fixed value $V_1=V_0-x'S$.

2.3 Model of porous material with rigid frame

Using the mathematic model presented above, it can establish some simple pneumatic exhaust system with expansion chamber muffler while seeming the connections between expansion chambers also as convergent nozzle. But in the dissipative mufflers, porous materials are always used to enhance the effect of sound absorption because of their favorable acoustic absorbing properties for suppressing noise [67]. Then a simple model of porous material with rigid frame is introduce.

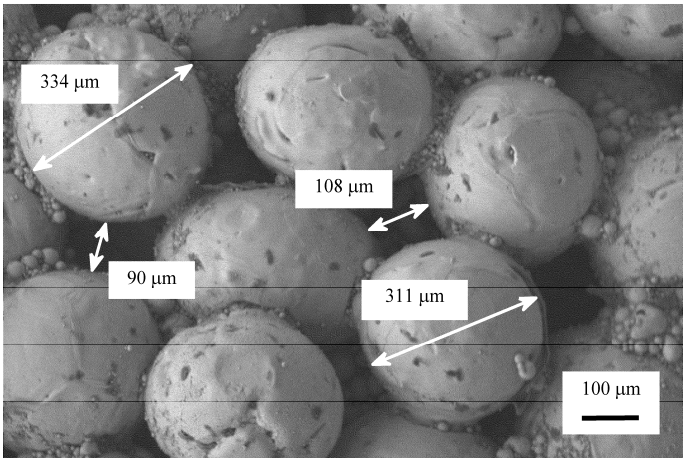

Figure 2-4 Micrographic surface of sintered bronze material. Note that the mean diameter of bronze particles is 320 μm, and the mean radius of pores is 50 μm.

As shown in Figure 2-4, the sintered bronze is a very common rigid porous material which is widely used to make silencers for the flow noise reduction. Differing from the traditional porous materials such as foams and mineral wool, sintered bronze retains the properties of metal such as heat transfer, high specific stiffness and intensity. It is particularly suitable for industrial applications under extreme conditions. The sintered bronze muffler is always sintered by the uniform bronze particles and is porosity allowing the air to flow through smoothly. Some

assumptions are listed as follows.

(1) It is isotropy inside the sintered bronze porous materials, and fully interconnected between all of the holes.

(2) The bronze particles are sphere with same size, ignoring the irregular shape and inhomogeneous distribution of particles.

(3) The sintered bronze materials are rigid both of the frame and the inside pore structure.

In order to study the aerodynamic properties of porous materials, Darcy-Forchheimer model is widely used to describe the relationship between pressure drop and flow velocity as the follow:

$$\frac{\Delta p}{L} = \frac{\mu}{\alpha} v_{\mathrm{s}} + C_2 \frac{1}{2} \rho v_{\mathrm{s}}^{\,2}, \tag{2-14}$$

where $\Delta p / L$ is the pressure drop per unit length of the porous material, μ and ρ are the dynamic viscosity and density of air, v_{s} is the superficial velocity (the average velocity over the flow cross-section), α is the permeability coefficient and C_2 is the inertial resistance factor. The dynamic viscosity μ can be obtained by Sutherland's formula.

Ergun equation is one form of Equation (2-14) which is widely used in the packed bed research of chemical engineering. For sintered bronze, the permeability α and inertial resistance factor C_2 can be described as follows[31]:

$$\alpha = \frac{D_{\mathrm{p}}^{\,2}}{150} \frac{\varphi^3}{(1-\varphi)^2}, \qquad C_2 = \frac{3.5}{D_{\mathrm{p}}} \frac{(1-\varphi)}{\varphi^3}, \tag{2-15}$$

where φ is the void fraction or the porosity (the ratio of the void volume and the total volume of the porous media), and D_{p} is the mean particle diameter about 320 μm as shown in Figure 2-4.

Considering the mass flow rate $\mathrm{d}m / \mathrm{d}t = \rho v_s S_s$ through the porous materials with the total superficial area of the material S_{s}, Equation (2-14) is rewritten as:

$$k_1\left(\frac{\mathrm{d}m}{\mathrm{d}t}\right)^2+k_2\frac{\mathrm{d}m}{\mathrm{d}t}-\frac{\Delta p}{L}=0\,, \tag{2-16}$$

with the coefficients $k_1=C_2/(2\rho S_s^{\,2})$ and $k_2=\mu/(\alpha\rho S_s)$. Therefore the mass flow rate can be solved from Equation (2-16) and remains positive while the back pressure is larger than the ambient pressure as:

$$\frac{\mathrm{d}m}{\mathrm{d}t}=\frac{-k_2+\sqrt{k_2^2+4k_1\Delta p/L}}{2k_1}\,. \tag{2-17}$$

In order to corroborate the validity of the presented model of sintered bronze materials, the flow property of volume flow vs. back pressure are calculated compared to the sample data of the sintered bronze silencer MS010A produced by Norgren Company with the parameters as particle diameter $D_p=320\,\mu\mathrm{m}$, porosity $\varphi=28\%$, thickness $L=2.6\,\mathrm{mm}$ and superficial area $S_s=0.0071\,\mathrm{m}^2$. The comparing results are shown in Figure 2-5[68].

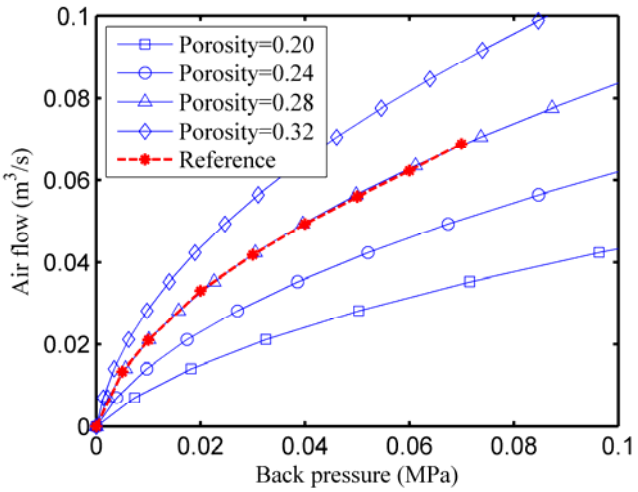

Figure 2-5 Flow property of sintered bronze silencer with different porosity. Blue lines are calculated according to the Ergun equation; Red line refers to the sample of real sintered bronze silencer (MS010A Norgren).

The porosity of the sintered bronze silencer MS010A was measured by density method, and

other parameters were measured directly. Figure 2-5 shows that the presented model of porous materials can describe the aerodynamic properties very well. Additionally, it can be seen that the volume flow increases with the pressure difference between the two sides of porous material; when the porosity increases, the flow resistivity will be reduced so that the air flow becomes more smooth.

2.4 Aerodynamic model of pneumatic exhaust systems

Combining the mathematic models presented above, the integrated aerodynamic model of a pneumatic exhaust system can be established. In the cases of direct exhaust system without silencer and exhaust system with a sintered bronze silencer, the whole models will be introduced in detail.

Figure 2-6 shows the simplified physical model of the direct exhaust system and the exhaust system with sintered bronze silencer. The direct exhaust system can be seem as a single-cylinder exhaust system; and the exhaust system with a sintered bronze silencer can be seem as a double-cylinders exhaust system with a porous material outlet.

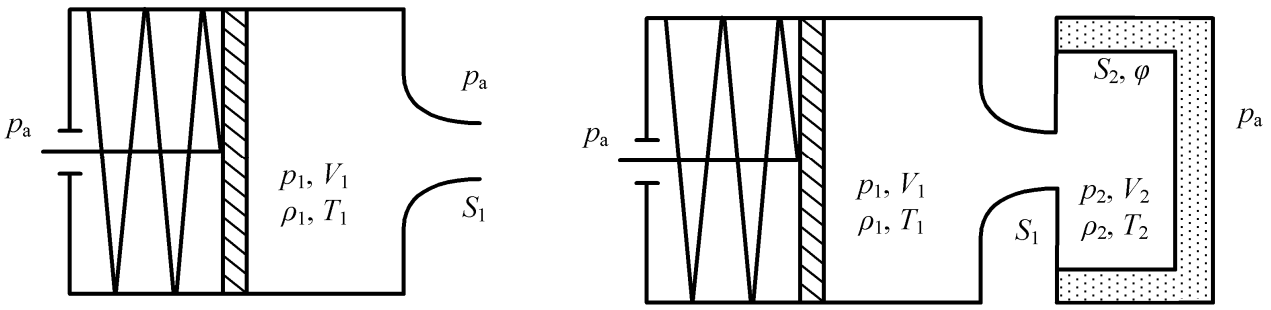

(a) Direct exhaust system (b) Exhaust system with sintered bronze silencer

Figure 2-6 Simplified physical model of pneumatic exhaust systems.

It is assumed that the gas parameters in the cylinder and silencer chamber are p_1, ρ_1, T_1, V_1 and p_2, ρ_2, T_2, V_2, and the initial parameters are p_{10}, ρ_{10}, T_{10}, V_{10} and p_{20}, ρ_{20}, T_{20}, V_{20}, respectively. Obviously, the initial parameters in the silencer chamber equal to environmental parameters. The integrated aerodynamic models of two pneumatic exhaust systems can be described as the following equations:

(1) Direct exhaust system

$$\begin{cases} \dfrac{\mathrm{d}p_1}{\mathrm{d}t} = f_1(t,\ p_1,\ V_1,\ S_1) \\ \dfrac{\mathrm{d}^2V_1}{\mathrm{d}t^2} = f_2(t,\ p_1,\ V_1,\ S_1) \qquad , \quad t>0 \\ \dfrac{\mathrm{d}S_1}{\mathrm{d}t} = f_3(t,\ p_1,\ V_1,\ S_1) \\ p_1(0) = p_{10},\ V_1(0) = V_{10},\ S_1(0) = 0 \end{cases} \tag{2-18}$$

(2) Exhaust system with sintered bronze silencer

$$\begin{cases} \dfrac{\mathrm{d}p_1}{\mathrm{d}t} = f_1(t,\ p_1,\ p_2,\ V_1,\ S_1) \\ \dfrac{\mathrm{d}p_2}{\mathrm{d}t} = f_2(t,\ p_1,\ p_2,\ V_1,\ S_1) \\ \dfrac{\mathrm{d}^2V_1}{\mathrm{d}t^2} = f_3(t,\ p_1,\ V_1,\ S_1) \qquad , \quad t>0 \\ \dfrac{\mathrm{d}S_1}{\mathrm{d}t} = f_4(t,\ p_1,\ V_1,\ S_1) \\ p_1(0) = p_{10},\ p_2(0) = p_{20} = p_{\mathrm{a}}, \\ V_1(0) = V_{10},\ S_1(0) = 0 \end{cases} \tag{2-19}$$

Therefore, the exhaust process can be established as initial value problems for ordinary differential equations (ODE). It can be solved by numerical methods such as Runge-Kutta scheme. The verification results are calculated by the codes in Matlab and compared with the experimental exhaust results, which are presented in Chapter 5.

Chapter 3 Sound sources and noise radiation analysis

In this chapter, the sound sources of impulse exhaust noise will be introduced according to the Lighthill's general theory, as the impulse exhaust noise is a kind of aerodynamic noise. The impulse exhaust noise is mainly composed of monopole sources related to the mass flow and quadrupole sources generated by the turbulence. Based on a piston sound source assumption, the noise radiation characteristics of the exhaust with sintered bronze muffler will be predicted. The mass flow considered as a monopole source is related to the sound pressure of impulse exhaust noise. And the sound pressure level (SPL) at a far-field observation point is predicted by the piston acoustic source approximation.

3.1 Lighthill's general theory of aerodynamic noise

The impulse exhaust noise is generated by the high pressure air discharging through the valve, pipes of pneumatic system. Due to the unsteady ejected mass, a simple monopole with sound strength Q is formed. The wave equation of impulsive exhaust is written as[21,22,29]

$$\frac{\partial^2 \rho}{\partial t^2} - c^2 \nabla^2 \rho = \frac{\partial Q}{\partial t} + \frac{\partial^2 T_{ij}}{\partial x_i \partial x_j}, \tag{3-1}$$

where T_{ij} is the Lighthill's stress tensor. Therefore, the source of transient exhaust noise is mainly composed of the monopole related to the mass flow and the quadrupole sources by turbulent flow[69-73].

The dimensions of pores at the superficial surface of the silencer are much smaller than the wavelength of the sound being radiated, therefore the sound sources can be act as point monopoles

approximately. An acoustic monopole radiates sound equally in all directions. In practice, the monopole can usually be regarded as a small sphere whose radius alternately expands and contracts. The sound pressure p in the far field which has a distance r from the sound source that $kr >> 1$ can be written by a monopole source as

$$p(r,t) = \frac{\rho_0}{4\pi r} \frac{\partial Q_{\mathrm{m}}(t - r/c_0)}{\partial t}, \tag{3-2}$$

where Q_{m} terms the complex sound strength and represents the volume flow rate. The relative time delay r/c_0 represents the sound arriving to the observation.

Considering the simple-harmonic source, the far-field sound pressure radiated by a single frequency point monopole may be written as

$$p_{\mathrm{m}}(r,\theta,t) = \frac{\mathrm{j}\omega\rho_0 Q_{\mathrm{m}}}{4\pi r} e^{\mathrm{j}(\omega t - kr)}, \tag{3-3}$$

and the pressure amplitude is then

$$\left| p_{\mathrm{m}}(r,\theta,t) \right| = \frac{\omega\rho_0 Q_{\mathrm{m}}}{4\pi r}, \tag{3-4}$$

where $k = \omega/c$ denotes the wave-number.

The quadrupole can be seemed as a combination of monopoles with different phase and separated by small distance d_{e}, related to the equivalent diameter of exhaust outlet that indicates the size of the source region. The far-field sound pressure radiated at the far-field point which is at the angle θ to the longitudinal axis by a quadrupole is written as

$$\left| p_{\mathrm{q}}(r,\theta,t) \right| = \frac{\omega\rho_0 Q_{\mathrm{m}}}{4\pi r} 4k^2 d_{\mathrm{e}}^2 \cos\theta \sin\theta. \tag{3-5}$$

So the amplitude of sound pressure produced by a quadrupole can be interpreted as the product of a simple monopole source, the dimensionless size term $4k^2 d_{\mathrm{e}}^2$, and the directivity function

$\cos\theta\sin\theta$. In particular, the amplitude of the quadrupole at specified frequency ω can be equivalent to $2k^2 d_e^{\,2}$ times that of the monopole when the observation point at 45° position as follows:

$$\left|p_q(r,\theta,t)\right| = \left|p_m(r,\theta,t)\right| 2k^2 d_e^2 . \tag{3-6}$$

That is to say, the quadrupole source can be equivalent to a monopole in far-field noise prediction mathematically.

3.2 Prediction of radiated exhaust noise

The radiated exhaust noise is closely related to the air flow especially at the outlet of pneumatic exhaust system. The sound pressure in the far-field can be calculated by the sound strength representing the monopole source of impulse exhaust. Furthermore, due to the relationship between the monopole and quadrupole sound source strength, the sound pressure at a far-field point can be predict. Then a prediction of the radiated exhaust noise based on the piston acoustic source assumption will be presented in details.

3.2.1 Piston acoustic source

The classical circular piston source in an infinite rigid baffle has been investigated by many authors[1]. The circular piston in an infinite rigid baffle, illustrated in Figure 3-1, is of interest because it has relatively simple geometry; it serves conveniently as an introduction to the behavior of all radiating surfaces; and it can be approximated by a speaker in a wall. The requirement that the baffle be infinite means that edges are far enough removed for diffraction effects originating there to be ignored. Alternatively, the edges of the baffle might be covered with a sound-absorbent

material with the same effect. Other authors have contributed about the classical circular piston source as well. Shi[7] applied this piston sound source to estimate the intermittent exhaust noise generated via a pneumatic value without silencers and have a reasonable prediction.

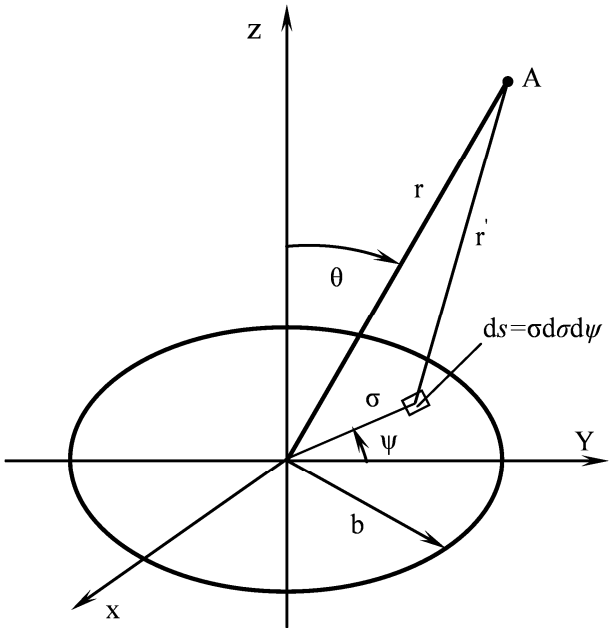

Figure 3-1 A piston source in an infinite baffle. The piston of radius a lies in the x - y plane and vibrates vertically parallel to the z-axis with velocity amplitude U .

3.2.2 Model of sintered bronze silencer

In this paper, the approximation of the piston sound source is applied to the impulse exhaust with a sintered bronze silencer shown in Figure 3-2 [68]. The simplified geometry of sintered bronze silencer is a cylindrical surface S_2 combining with a round bottom S_1 as shown in Figure 3-3. In this simplified model, the transient exhaust flows into the chamber of silencer and then discharges through the round surface S_1 and cylindrical surface S_2 to the environment. Considering that the radiated noise at both the round bottom and cylindrical surface are approximated seemed as piston acoustic sources, just as a speaker in a wall, the formula of

predicting SPL of the observation point A at a distance r from the outlet of ducts and at an angle θ to the longitudinal axis will be derived in detail.

Figure 3-2 Photos of sintered bronze silencer.

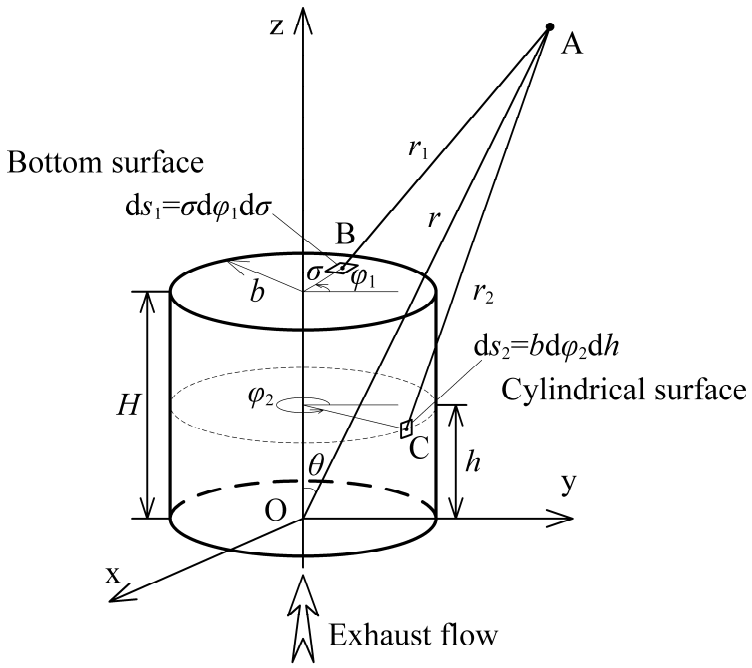

Figure 3-3 Piston acoustic sources at the superficial surfaces of sintered bronze silencer. The circular approximated piston S_1 of radius b and cylindrical approximated piston S_2 vibrate perpendicularly to the surfaces with velocity amplitude U_0.

Reference to Figure 3-2, the distance r_1 of observation point A from the source B is given by the following expression in terms of the centre-line distance r:

$$r_1 = (r^2 + \sigma^2 + H^2 - 2rH\cos\theta - 2r\sigma\sin\theta\cos\varphi_1)^{1/2} . \quad (3\text{-}7)$$

For the case of far field where $r >> 2b$ and $r >> 2H$, Equation (3-7) becomes approximately:

$$r_1 \approx r - H\cos\theta - \sigma\sin\theta\cos\varphi_1 . \quad (3\text{-}8)$$

The distance r_2 of observation point A from the source C at the cylindrical surface can also be given as the similar expression of Equation (3-8) as:

$$r_2 \approx r - h\cos\theta - b\sin\theta\cos\varphi_2 . \quad (3\text{-}9)$$

The further simplification may be made while substituting Equation (3-8) and Equation (3-9) into Equation (3-4) that the denominator is approximated sufficiently by the first term on the right-hand side of the two distance equations. However, the last two terms must be retained in the exponent, which reflects the fact that small variations in relative phase of the pressure contributions arriving at the observation point have a very significant effect upon the sum [1,8,74].

3.2.3 Prediction of radiated exhaust noise

The hypothetical pistons in rigid baffles, generally restricted to a circle S_1 of radius b and a cylindrical surface S_2 of radius b and height H, are assumed to vibrate with uniform normal velocity $U = U_0 e^{j\omega t}$ harmonically of amplitude U_0 and angular frequency ω. The presence of the baffles implies that all of the sound power radiated by the pistons is radiated into the hemispherical half-space bounded by the planes of the baffles. Therefore the amplitudes of the

strength of the sources corresponding to the incremental areas $\mathrm{d}S_1 = \sigma \mathrm{d}\varphi_1 \mathrm{d}\sigma$ and $\mathrm{d}S_2 = b\mathrm{d}\varphi_2 \mathrm{d}h$ are

$$Q_{\mathrm{m1}} = 2U_0 \sigma \mathrm{d}\varphi_1 \mathrm{d}\sigma\,, \quad Q_{\mathrm{m2}} = 2U_0 b \mathrm{d}\varphi_2 \mathrm{d}h\,, \tag{3-10}$$

respectively, of which the factor 2 is introduced to express that the noise radiates only hemispherically due to the presence of the rigid pistons.

Considering contributions from all points over the piston surface, the total pressure at the far-field observation point A radiated by the circular surface S_1 is given as the following integral expression:

$$p_{\mathrm{m1}}(r,\theta,t) = \frac{\mathrm{j}\omega\rho_0 U_0}{2\pi r} e^{\mathrm{j}(\omega t - kr)} e^{\mathrm{j}kH\cos\theta} \int_0^b \sigma \int_0^{2\pi} e^{\mathrm{j}k\sigma\sin\theta\cos\varphi_1} \mathrm{d}\varphi_1 \mathrm{d}\sigma\,, \tag{3-11}$$

which can be derived to a simple expression by the Bessel function as:

$$p_{\mathrm{m1}}(r,\theta,t) = \frac{\mathrm{j}\omega\rho_0 U_0 b^2}{r} e^{\mathrm{j}(\omega t - kr)} e^{\mathrm{j}kH\cos\theta} \left(\frac{\mathrm{J}_1(kb\sin\theta)}{kb\sin\theta} \right). \tag{3-12}$$

The similar result of the total pressure at the far-field observation point A radiated by the cylindrical surface S_2 is of the form:

$$\begin{aligned} p_{\mathrm{m2}}(r,\theta,t) &= \frac{\mathrm{j}\omega\rho_0 U_0}{2\pi r} e^{\mathrm{j}(\omega t - kr)} \int_0^H b e^{\mathrm{j}kh\cos\theta} \int_0^{2\pi} e^{\mathrm{j}kb\sin\theta\cos\varphi_2} \mathrm{d}\varphi_2 \mathrm{d}h \\ &= \frac{\omega\rho_0 U_0 b^2}{r} e^{\mathrm{j}(\omega t - kr)} \left(e^{\mathrm{j}kH\cos\theta} - 1 \right) \left(\frac{\mathrm{J}_0(kb\sin\theta)}{kb\cos\theta} \right) \end{aligned}. \tag{3-13}$$

The quantities $\mathrm{J}_0(kb\sin\theta)$ and $\mathrm{J}_1(kb\sin\theta)$ are Bessel functions of the first kind of order 0 and 1, respectively. Comparing Equation (3-12) and Equation (3-13), the difference of imaginary unit $\mathrm{j} = (-1)^{1/2}$ represents that the directions of two piston surfaces are perpendicular to each other. With the Fourier transform, SPL in frequency-domain at the far-field observation point A radiated

by the two piston surfaces can be calculated respectively, and read

$$L_{\mathrm{Pm1}} = 10\log_{10}\left(\left(\frac{\omega\rho_0 U_0(\omega)b^2}{rp_{\mathrm{r}}}\left(\frac{\mathrm{J}_1(kb\sin\theta)}{kb\sin\theta}\right)\right)^2\right),$$
$$L_{\mathrm{Pm2}} = 10\log_{10}\left(\left(\frac{\omega\rho_0 U_0(\omega)b^2}{rp_{\mathrm{r}}}\left(e^{\mathrm{j}kH\cos\theta}-1\right)\left(\frac{\mathrm{J}_0(kb\sin\theta)}{kb\cos\theta}\right)\right)^2\right), \tag{3-14}$$

where $p_{\mathrm{r}} = 20\,\mu\mathrm{Pa}$ is the reference sound pressure in the air, $U_0(\omega)$ is the Fourier transform of the amplitude of normal vibration velocity of the pistons that is the superficial velocity v_{s} of the transient exhaust flowing through the sintered bronze porous material.

For the noise radiated by the two equivalent quadrupoles mentioned above in Equation (3-6), SPL L_{Pq1} and L_{Pq2} at the far-field observation point A will be calculated using the similar expressions of Equation (3-14).

Therefore the prediction of total SPL containing the effects of monopoles and quadrupoles of the two hypothetical piston surfaces can use the following formula:

$$L_{\mathrm{P}} = 10\log_{10}(10^{L_{\mathrm{Pm1}}/10} + 10^{L_{\mathrm{Pm2}}/10} + 10^{L_{\mathrm{Pq1}}/10} + 10^{L_{\mathrm{Pq2}}/10}). \tag{3-15}$$

Chapter 4 Strategies of impulse exhaust noise suppression

In this chapter, the control strategies of impulse exhaust noise will be presented. There are three approaches to control the noise from the sound source, the propagation path and the receiver, respectively. Muffler devices are used to reduce the aerodynamic jet noise classically. The features and disadvantages of various mufflers in the industrial applications will be introduced firstly. Unlike the steady noise or period noise, the evaluations of impulse noise is introduced. Then a semi-active control strategy to change the sound source of impulse exhaust by controlling the opening process of exhaust valve is presented. The principle and specific control method will be introduced.

4.1 Classical control strategy

In order to suppress the exhaust noise, workers may wear the earplug in factories as the earplug can weaken most of the high-frequency noise. However, wearing the earplug may affect the hearing and conversation between peoples, so many workers do not like to use it. Mufflers as the most frequently-used devices to control the aerodynamic noise, are commonly installed at the outlet of exhaust systems by reflection or absorption of sound. There are several kinds of mufflers or silencers. Expansion chamber mufflers as the simplest reactive muffler suddenly expand and reduce the cross-section area to reflect the sound wave back to the source and reduce the amount of acoustic energy transmitted. Unlike reactive mufflers, absorptive mufflers which incorporate sound absorbing porous materials such as fiberglass, mineral wool and high-porosity foams to transform acoustic energy into heat. Absorbing materials have some disadvantages including pollution, the risk of high heat and limited lifetime therefore they may become ineffective and impractical.

Nevertheless, the porous mufflers are widely used in the pneumatic exhaust noise reduction because of the desirable characteristics for broadband noise. Perforated panel with wide absorption sound spectrum and high sound absorption coefficient was studied and applied to suppress the industrial noise in recent decades. Muffling devices may suppress the generation of noise or attenuate noise already generated passively on the noise propagation path; but they are designed for specific equipment and might impede the exhaust, especially the dissipative mufflers. Alternatively, it can become a serious source of noise if attention is not given to the design.

4.2 Semi-active control strategy

Although the mufflers are widely used in the industrial noise control, they are basically designed according to the theories of reducing noise generated by the steady exhaust or period exhaust. The impulse exhaust noise has a obvious unsteady characteristic due to the short impulse exhaust, which is different from the steady noise or the period noise. It should pay close attention to reduce not only the overall A-weighted SPL or the SPL in frequency but also the peak sound pressure in time-domain.

4.2.1 Evaluations of impulse noise

The sensitivity of the human ear to sound (perceived sound) not only varies with the magnitude (measured physically by a microphone) but also with the frequency. The apparent loudness of a sound varies with frequency as well as with sound pressure. The variation of loudness with frequency also depends to some extent on the sound pressure. The A weighted SPL is widely used in assessing loss of hearing causing by the noise in industries due to its good approximation of

the ear response. There are several types of measurements to evaluate the impulse noise, such as A-weighted equivalent level L_{Aeq}, the peak sound pressure [19].

The magnitude of the continuous signal like steady or fluctuating noise can be generally expressed by an effective value which is based upon mean square value of signals. The quantity L_{Aeq} is the equivalent continuous A-weighted noise level, which characterizes fluctuating noise as an equivalent steady-state level and is defined as:

$$L_{\mathrm{Aeq}} = 10\log_{10}\frac{1}{T_0}\int_0^{T_0} 10^{L_{\mathrm{pA}}(t)/10}\mathrm{d}t \quad \mathrm{dB(A)} \tag{4-1}$$

where T_0 is a reference time and $L_{\mathrm{pA}}(t)$ is the A-weighted sound pressure level at time t.

However, the time-mean concept may not be applicable to an impulse noise because of its short duration time. Thus it seems physically plausible that the total energy $E(t)$ of an impulse signal $x(t)$ should be used for assessment of noise. As shown in Figure 4-1, the equivalent energy can be given as a height of the square pulse $e = E(t)/T_0$. In order to make it physically more clear, we can express a height of square pulse as a sound level L_{pe} (dB), defined as:

$$L_{\mathrm{pe}} = 10\log_{10}\frac{1}{T_0}\int_0^{\infty}\frac{x^2(t)}{e_0}\mathrm{d}t \tag{4-2}$$

where e_0 is a reference value (sound pressure of $(2\times10^{-5}\ \mathrm{Pa})^2$) and T_0 is a reference time. There are some different ways in determining T_0, but $T_0 = 1\ \mathrm{s}$ is generally accepted as a unit time.

In assessment of impulse noise, ISO (ISO 1996/1) also uses the same concept mentioned above. This is illustrated in Figure 4-2. A sound exposure level L_{ae} (dB(A)) can be expressed similar to Equation (4-2) as

$$L_{ae} = 10\log_{10}\left(\frac{1}{T_0}\int_{t_1}^{t_2}\frac{p_a{}^2(t)}{p_0^2}\mathrm{d}t\right) \tag{4-3}$$

where T_0 is a reference time ($T_0 = 1\,\mathrm{s}$), the interval between t_1 and t_2 indicating a duration time of single impulse noise, $p_a(t)$ and p_0 are an A-weighted sound pressure and a reference sound pressure (2×10^{-5} Pa), respectively. The time $\Delta t = t_2 - t_1$ is defined as the duration time of impulse noise required for the peak level to drop 20 dB.

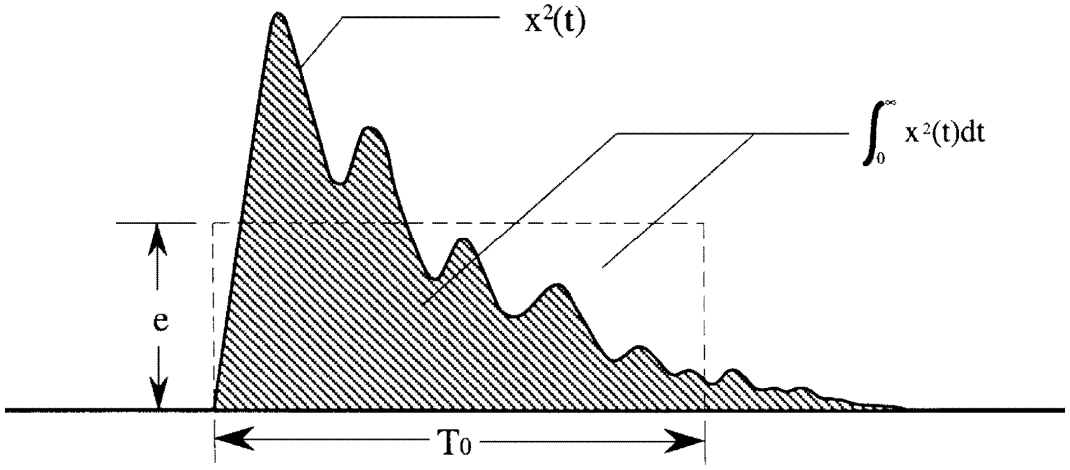

Figure 4-1 Energy of impulse signal.

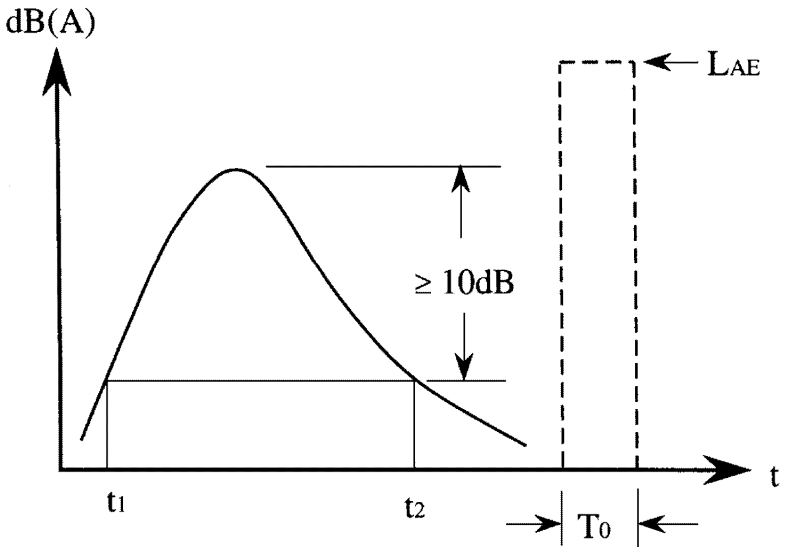

Figure 4-2 Sound exposure level of impulse signal.

If the noise data in time series are sampled at a time interval being sufficiently short compared with the duration time of noise, then L_{pe} can be obtained by the following equation

$$L_{pe} = 10\log_{10}\frac{\Delta t}{T_0}\sum_{t=1}^{n}10^{L_p(t)/10} \tag{4-4}$$

where $L_p(t)$ and n are the sound pressure value of each sample and the total number of sample, respectively. It should be noted that, in this case, the sampling interval of data must be taken to be sufficiently short compared with the averaging time. In this paper, the impulse exhaust noise is sampled in 50 kHz and the total time is 1 s as equal to the reference time T_0, according with the condition mentioned above.

4.2.2 Principle

The impulse noise with high peak sound pressure is harmful to people and may cause hearing damage. Thus, the suppression of peak sound pressure of impulse noise is the mainly purpose in this section. It is known that the impulse exhaust noise is closely related of the transient exhaust flow, and the peak sound pressure always occurs at the sonic exhaust stage, which is the very beginning of the exhaust process because of the obvious pressure difference and suddenly huge amount air flow. That is the focus stage requiring suppression at the time sonic choked exhaust happens.

Considering an impulse exhaust process of a fixed volume cylinder without silencer, the sound pressure reaches the peak value when the mass flow rate is maximum as shown in Figure 4-3, the measured cylinder pressure and sound noise signals during the impulse exhaust process. The mass flow rate is calculated by Equation (2-7) and Equation (2-9). The figure also shows that the envelope of noise signal is closed to the vary of mass flow rate at the throat of valve.

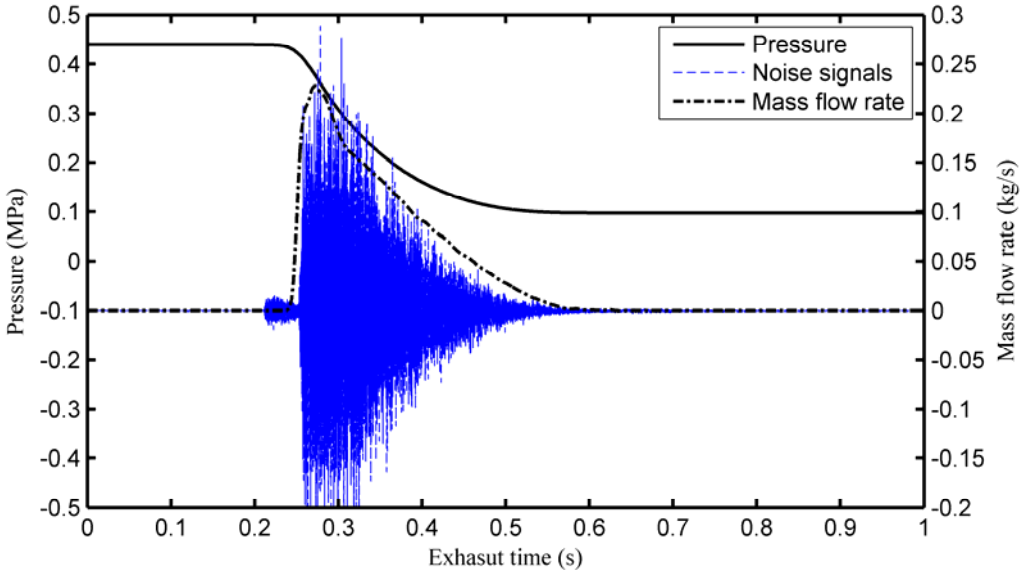

Figure 4-3 The cylinder pressure, noise and mass flow rate of impulse exhaust.

Focusing on the sonic exhaust stage, the pressure derivate can be obtained by Equation (2-4), Equation (2-7) and Equation (2-9) as follows:

$$\begin{cases} \dfrac{\mathrm{d}p_\mathrm{c}}{\mathrm{d}t} = -\left(\dfrac{2}{\gamma+1}\right)^{1/(\gamma-1)} \dfrac{S_\mathrm{v}}{V_\mathrm{c}} \left(\dfrac{2\gamma^3 RT_{\mathrm{c0}}}{\gamma+1}\right)^{1/2} p_{\mathrm{c0}}^{(1-\gamma)/(2\gamma)} p_\mathrm{c}^{(3\gamma-1)/(2\gamma)}, & p_\mathrm{c} \geq p^* \\ \dfrac{\mathrm{d}p_\mathrm{c}}{\mathrm{d}t} = -\dfrac{S_v}{V_\mathrm{c}} p_{\mathrm{c0}}^{(1-\gamma)/(2\gamma)} p_\mathrm{c}^{(3\gamma-1)/(2\gamma)} \left[\dfrac{2\gamma^3 RT_{\mathrm{c0}}}{(\gamma-1)} \left(\left(\dfrac{p_\mathrm{a}}{p_\mathrm{c}}\right)^{2/\gamma} - \left(\dfrac{p_\mathrm{a}}{p_\mathrm{c}}\right)^{(\gamma+1)/\gamma}\right)\right]^{1/2}, & p_\mathrm{c} < p^* \end{cases} \quad (4\text{-}5)$$

where p_c and T_c are the pressure and temperature of air inside the cylinder, p_{c0} and T_{c0} are initial values, V_c is the cylinder volume, and S_v is the effective cross-sectional area of the valve throat, p^* is the critical pressure ($p^* = \left[(\gamma+1)/2\right]^{\gamma/(\gamma-1)} p_\mathrm{a}$). Therefore, the pressure of cylinder is a function of the valve throat area $S_\mathrm{v}(t)$ when the initial condition is fixed. In other words, the exhaust process is according to the different opening process of valve.

In order to suppress the peak sound pressure of exhaust noise, the maximum of mass flow rate should be limited. The total mass exhaust from the cylinder is almost same if the initial pressure

inside the cylinder is fixed because of the exhaust process is seemed as isentropic. Therefore, if the mass flow rate keeps a steady value during the exhaust process, the form of mass flow rate is like a square and the peak of impulse noise will be reduced maximally. According to Equation (2-4), the mass flow rate can be derived as

$$\frac{\mathrm{d}m}{\mathrm{d}t} = -\frac{V_\mathrm{c}}{\gamma R T_\mathrm{c}} \frac{\mathrm{d}p_\mathrm{c}}{\mathrm{d}t} . \tag{4-6}$$

Neglecting the temperature changes compared with the derivative of cylinder pressure, the mass flow rate is approximatively proportional to the cylinder pressure derivative. Therefore, the maximum of mass flow rate and the peak sound pressure of exhaust noise can be limited when the cylinder pressure decreases linearly. The schematic diagram of principle is illustrated in Figure 4-4.

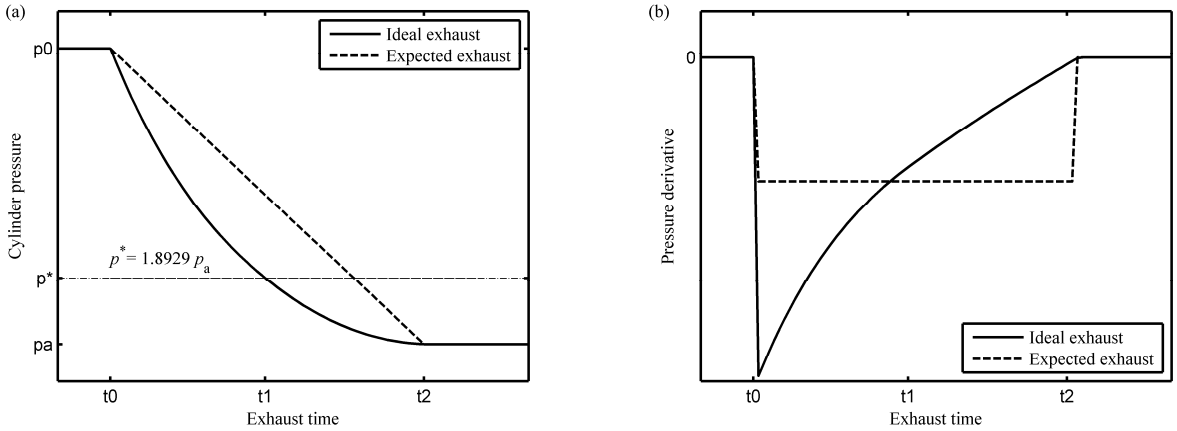

Figure 4-4 The schematic diagram of semi-active control strategy.

(a) The pressure curves of the ideal impulse exhaust and expected exhaust; (b) The pressure derivative curves of the ideal impulse exhaust and the expected exhaust.

The ideal cylinder pressure during the impulse exhaust process is shown as the solid line if the effective cross-sectional area of valve throat is constant. The impulse exhaust starts from time t_0, before which the pressure of cylinder keeps the initial value p_0. The cylinder pressure decreases

rapidly in the sonic exhaust stage from the initial pressure p_0 to the critical pressure p^* at time t_1, and softly in the subsonic exhaust until the ambient pressure at time t_2. The derivative of pressure suddenly steps to the peak value at the beginning of exhaust, then decreases gradually during the sonic exhaust stage as the power function presented in Equation (4-5). This also proves the transient peak value of impulse noise reaches at the initial stage. After that, the derivative of pressure continues to decrease but according to a more complex raw as Equation (4-5) for the subsonic exhaust process. If the cylinder pressure decreases linearly as the dash line, the pressure derivative will be a constant. Furthermore, the mass flow rate approximately being proportional to the pressure derivative in the sonic exhaust stage will be limited to minimum so that the flow noise due to the unsteady mass flow can be reduced and the peak of sound pressure may keep stable.

4.2.3 Control method

The principle of semi-active control strategy for suppressing the impulse exhaust noise is to linearize the cylinder pressure by controlling the opening process of valve. When the initial state parameters of air inside the cylinder are known and the expected exhaust time Δt is chosen, the linearized pressure during the exhaust process can be obtained by the following expression as:

$$p(t) = p_0 - \frac{p_0 - p_a}{\Delta t}(t - t_0). \tag{4-7}$$

In accordance with Equation (4-5), the effective cross-sectional area of valve throat can be given as a variable to ensure the cylinder pressure decreasing as expected. Here we should also consider the saturation value of area due to the structure of valve.

Chapter 5 Experimental study

In this chapter, experimental study will be presented. The experiments were based on a pneumatic friction clutch and brake (PFC/B) system of mechanical press and also a simplified cylinder exhaust system. In order to test the presented semi-active noise control strategy, a modified pneumatic valve was designed, which can adjust the poppet valve by a servo motor. The experimental results will be shown to verify the validity of the presented aerodynamic model and the radiated noise predictions. The noise were analyzed to study the effect of presented suppression strategy comparing to the direct exhaust.

5.1 Experimental apparatus

5.1.1 PFC/B test-bed

The experiment was based on a PFC/B system of JH23-63 mechanical press as shown in Figure 5-1. Without silencer and with a sintered bronze silencer installed at the outlet of valve, the cylinder pressure and the exhaust noise were measured by a pressure sensor and a microphone with sound level meter. The real exhaust system was set in a large room (7 × 7 × 6 m) including an acting cylinder, a hybrid regulator valve VY1700, exhaust pipes, a sintered bronze silencer MS010A as shown in Figure 3-2, a pressure sensor GB-3000A, a sound level meter Type 2270 with microphone 4189, etc. The microphone was fixed at a distance of 1 m from the silencer and at an angle of 45° to the longitudinal axes of the exhaust outlet. The sensitivity of sound level meter is 47.57 mV/Pa. Both the cylinder pressure and exhaust noise signals were recorded by a 12 bit A/D converter multifunction card PCI-1712 with 200 kHz sampling rate. In addition, the experiments

were tested in night with the background noise less than 30 dB for ignoring the influence of environmental disturbance.

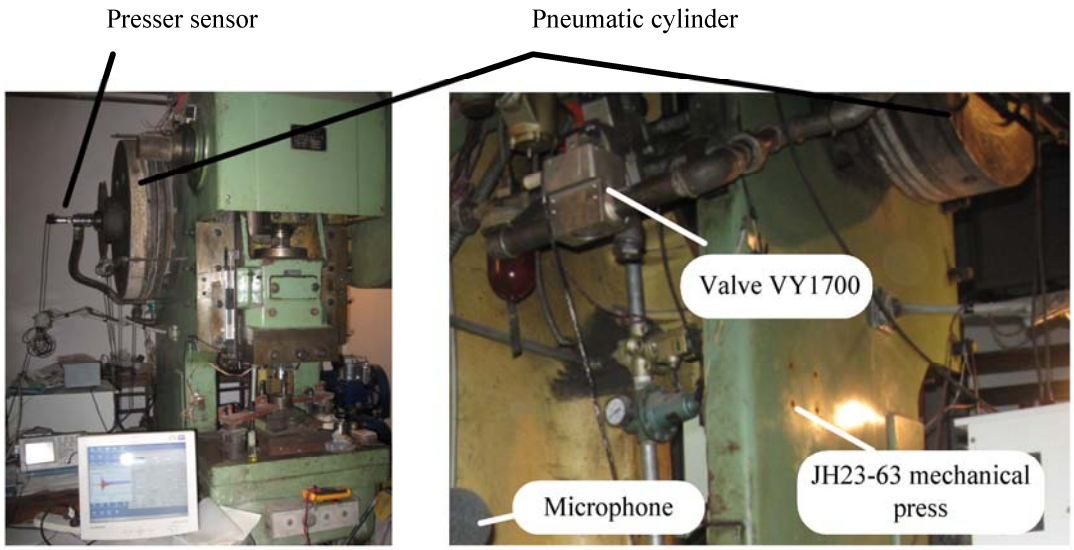

Figure 5-1 Pneumatic exhaust system based on a PFC/B system of JH23-63 mechanical press.

5.1.2 Modified pneumatic valve

In order to test and verify the semi-active noise control strategy presented in Chapter 4, a 3/2-way directional valve was modified, of which the schematic diagram is shown in Figure 5-2. The modified pneumatic valve is composed of a servo motor, a ball-screw pair, poppet valves, a valve body and covers. When the poppet valve moves downward to the position as shown in Figure 5-2, the air from port P is supplied into port A. Conversely, when the poppet valve moves upward, the passage between port P and port A is closed, but allowing the air to be discharged from port A to port R. Different from the ordinary pneumatic directional valve driven by a pilot solenoid valve, the modified valve is driven by a servo motor. The rotation of motor is converted into linear movement of poppet valve by the ball-screw unit. This is a kind of half-open-loop control system. Thus, the poppet valve can be adjusted accurately by the position control of servo motor. The displacement of

poppet valve is obtained by the integral of the encoder pulse signals.

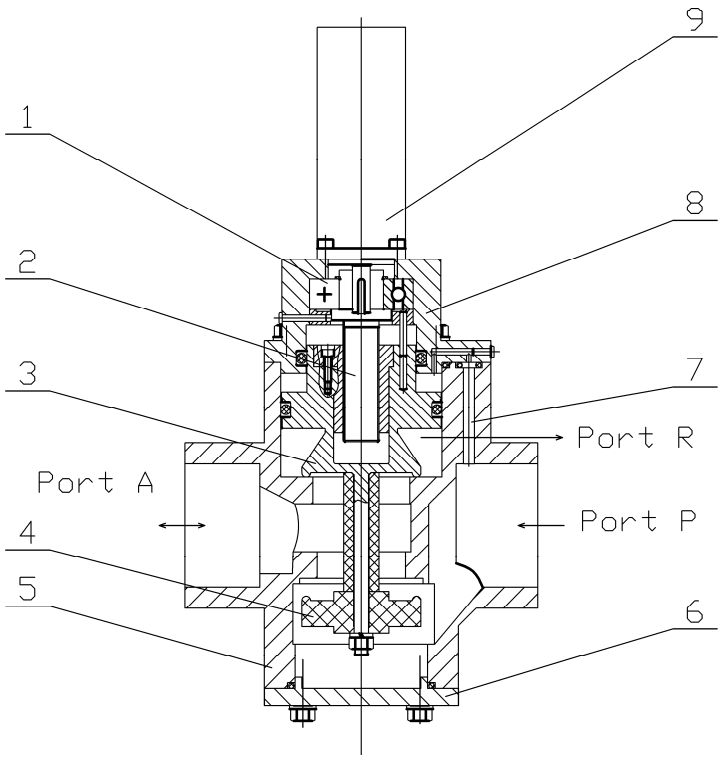

Figure 5-2 Modified pneumatic valve. It includes 1-bearing; 2-ball-screw pair; 3-poppet valve; 4-poppet valve; 5-body; 6-cover; 7-feed back passage; 8-cover; 9-servo motor.

5.1.3 Simplified cylinder exhaust test-bed

The simplified cylinder exhaust test-bed was based on a simple pneumatic system composed of an air compressor, an air treatment device including filter, relief valve and lubricator (FRL), a 3/2-way directional valve and a cylinder as shown in Figure 5-3. The system was set in a large room in order to simulate the real environment in an application. A pressure sensor GB-3000A was installed at the duct near the cylinder to measure the cylinder pressure. A microphone 4189 connected with a sound level meter Type 2270 was placed at a distance of 1 m and at an angle of 45° to the longitudinal axes of the valve outlet to measure and record the impulse exhaust noise.

The valve position was obtained by the counting of motor encoder signals. All of the experimental data were recorded by a high-speed A/D converter multifunction card PCI-1712 with 50 kHz sampling rate. Additionally, the background sound was 30 dB much lower than the exhaust noise when the experiments were carried out at night.

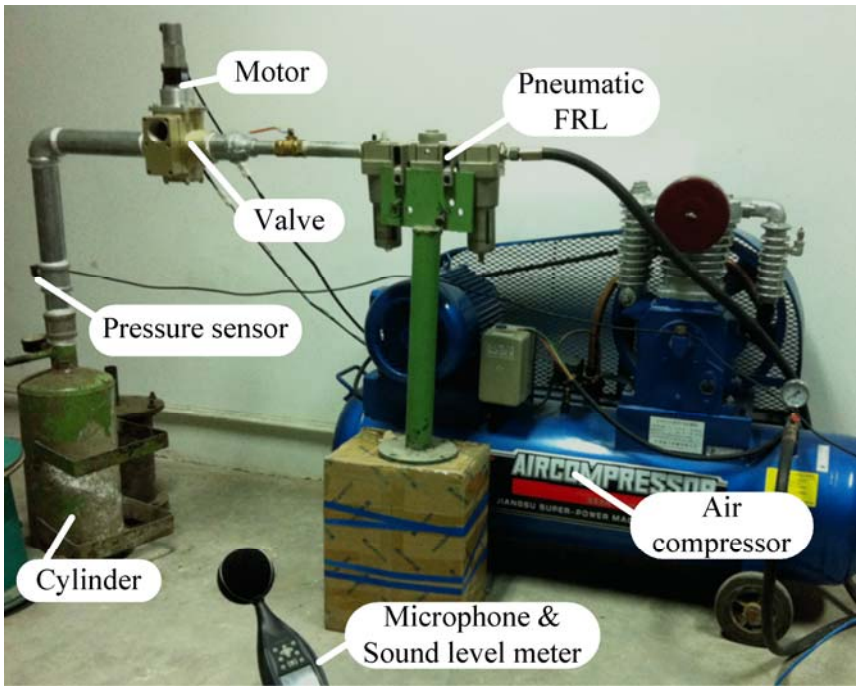

Figure 5-3 Simplified exhaust system. The volume of cylinder is fixed.

5.2 Results of aerodynamic model

The experiments were carried out based on the introduced PFC/B test-bed to verify the aerodynamic models of impulse exhaust process and porous material with rigid frame presented in Chapter 2. Experiments measured the cylinder pressures of the exhaust system which exhausted directly and with a sintered bronze silencer, respectively. The exhaust processes under some different initial cylinder pressure conditions were tested, of which the results are presented and discussed in details.

5.2.1 Direct exhaust without silencer

According to the aerodynamic model of direct exhaust by PFC/B exhaust system, the initial value problem for ODE as equation (2-17) can be solved by using the ode functions of Matlab (e.g. ode45). Thus, the parameters of the direct exhaust process are obtained. Figure 5-4 shows the cylinder pressures with different initial conditions, that the initial pressures in the cylinder are 0.36 MPa and 0.48 MPa, respectively. The pressure reduces to the ambient pressure ($p_a = 0.0968$ MPa) in a very short time, less than 0.13 s. At the beginning of exhaust, the cylinder pressure derivative increases gradually due to the change of effective cross-sectional area of the valve VY1700. When the cylinder pressure decreases at about 0.15 MPa, the speed of pressure drop increases because the piston begins to move to reduce the volume of cylinder. The errors of calculated cylinder pressure compared to the experimental results are about 4.6 percent for the maximum value and less than 1.6 percent for the mean absolute value. That verifies the applicability of the presented aerodynamic model of impulse exhaust through pneumatic valve.

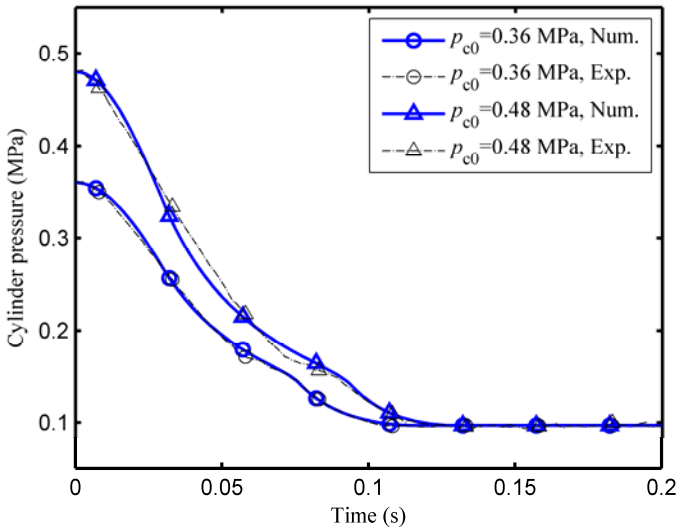

Figure 5-4 Cylinder pressure of direct exhaust process.

In order to analyze the aerodynamic properties of impulse exhaust, some difficulty measured parameters can also calculated by the mathematic model of direct exhaust, such as mass flow rate and mach number at the throat of valve. Figures 5-5 and 5-6 show the calculated results of mass flow rate and mach number at the valve throat under different initial pressures 0.36 MPa and 0.48 MPa. Because of the opening response of valve, the mass flow rate shown in Figure 5-5 increases when the exhaust starts, although the mach number at the valve throat shown in Figure 5-6 reaches 1 at the same time. The higher initial pressure of cylinder means that there are more air will exhaust through the valve. Therefore, the total quality of exhaust air, as the integral of mass flow rate curve, will be larger and the exhaust will takes longer time when the air inside the cylinder has a higher initial pressure. Comparing Figures 5-4 and 5-6, when the cylinder pressure is larger than the critical value $1.8929 p_a$, the sonic choked exhaust happens and the mach number at the valve throat equals to 1. In addition, it can be seen clearly from Figure 5-6 that the higher initial pressure will extend not only the total exhaust but also the sonic choked exhaust process.

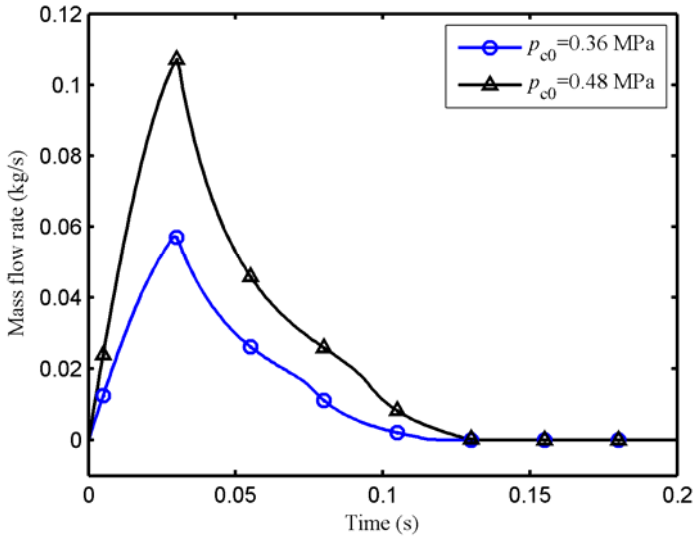

Figure 5-5 Mass flow rate at the valve throat of direct exhaust process.

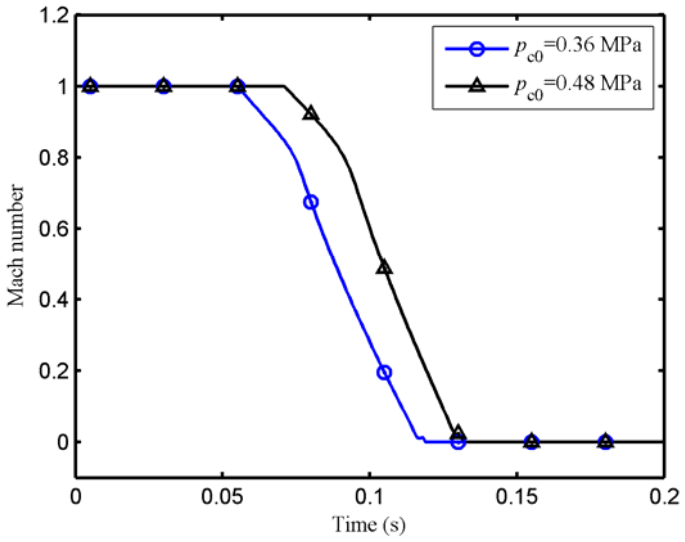

Figure 5-6 Mach number at the valve throat of direct exhaust process.

5.2.2 Exhaust with sintered bronze silencer

According to the simplified aerodynamic model of pneumatic system with sintered bronze silencer established above, the parameters of the exhaust process are also calculated by using the ode functions in Matlab. Figure 5-7 shows the comparison of the measured and calculated pressure of the pneumatic cylinder with different initial pressures: 0.36 MPa and 0.48 MPa. The pressure reduces to the ambient pressure in a short time, which is little longer than that of direct exhaust process. The calculated results with the maximum error of about 4.4 percent and the mean absolute error less than 2 percent confirm to the actual exhaust process at different initial conditions, which verifies the applicability of the presented aerodynamic models of impulse exhaust and porous material with rigid frame.

As same as the analysis of direct exhaust, the mass flow rate through the sintered bronze silencer is also calculated by the aerodynamic model with the Ergun equation, as shown in Figure 5-8. The mass flow rate increases rapidly in the early stage and gets the peak, the time taken for

which is about 28 ms which is independent of the initial cylinder pressure. Then it reduces until the end of the exhaust process since the cylinder pressure decreases. Nevertheless, the integral of the mass flow rate represents the total quality of exhaust air from the pneumatic cylinder, and is related to the initial cylinder pressure obviously.

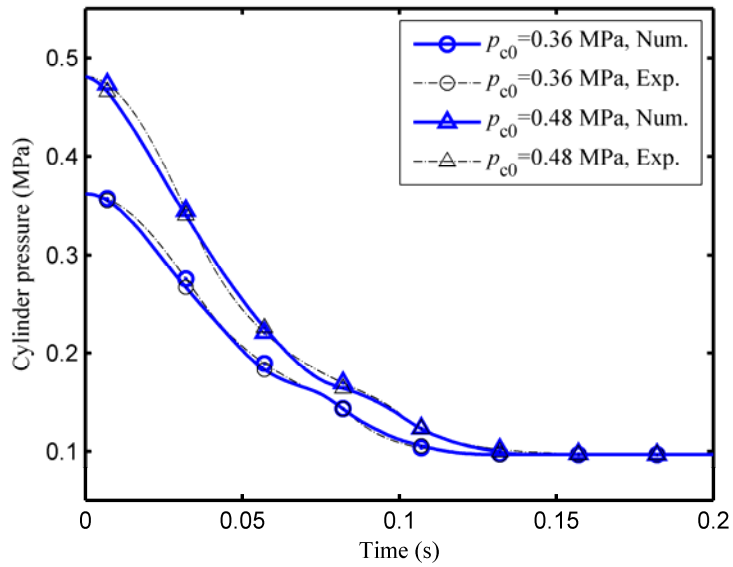

Figure 5-7 Cylinder pressure of exhaust process with sintered bronze silencer.

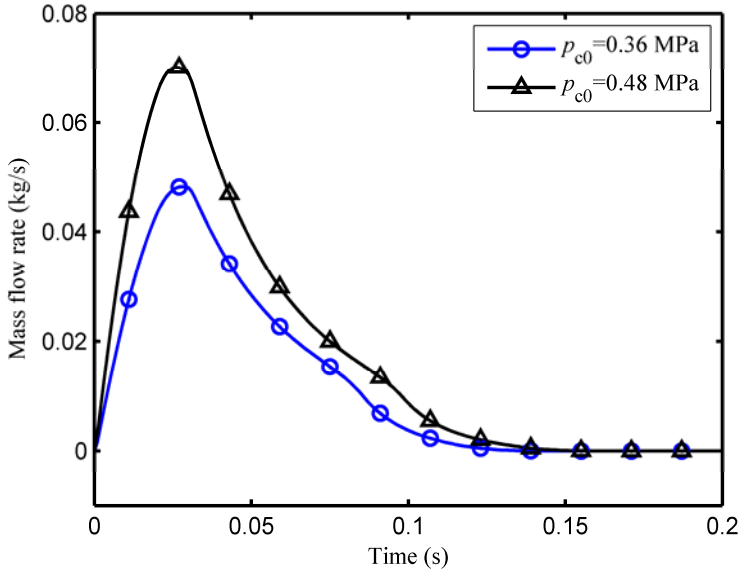

Figure 5-8 Mass flow rate at the valve throat of exhaust process with sintered bronze silencer.

It can be seen from the above discussions, the presented aerodynamic model can used to analyze the flow properties of the impulse exhaust and also of the porous material with rigid frame. The results are reasonable so that according to the mathematic model, we can have a more in-depth understanding of the impulse exhaust process.

5.3 Results of radiated noise prediction

Based on the previous discussions, the primary monopole and quadrupole sources of transient exhaust noise can be related to the mass flow rate and other parameters. The flow parameters can be calculated by the aerodynamic model. Therefore, the sound pressure of the radiated acoustic field at far field (1 m in the experiments) can be predicted. The noise signals generated by the impulse exhaust of PFC/B exhaust system with a sintered bronze silencer were recorded and analyzed to verify the applicability of presented prediction theory of radiated noise.

5.3.1 Noise prediction in time-domain

Figure 5-9 shows the relationship between the acquired noise signal and the calculated sound pressure related to the flow parameters through the sintered bronze silencer in time-domain. In order to compare conveniently, the noise signals are shifted 2.94 ms forward to counteract the sound propagation time. It is shown that the predicted results are similar with the upper envelope of the noise signal at different initial pressures. Both the magnitude and the peak time of calculated sound pressure are matched well. Therefore, the flow parameters can be used to predict the sound pressure and reflect the magnitude information of the impulse exhaust noise to a certain degree.

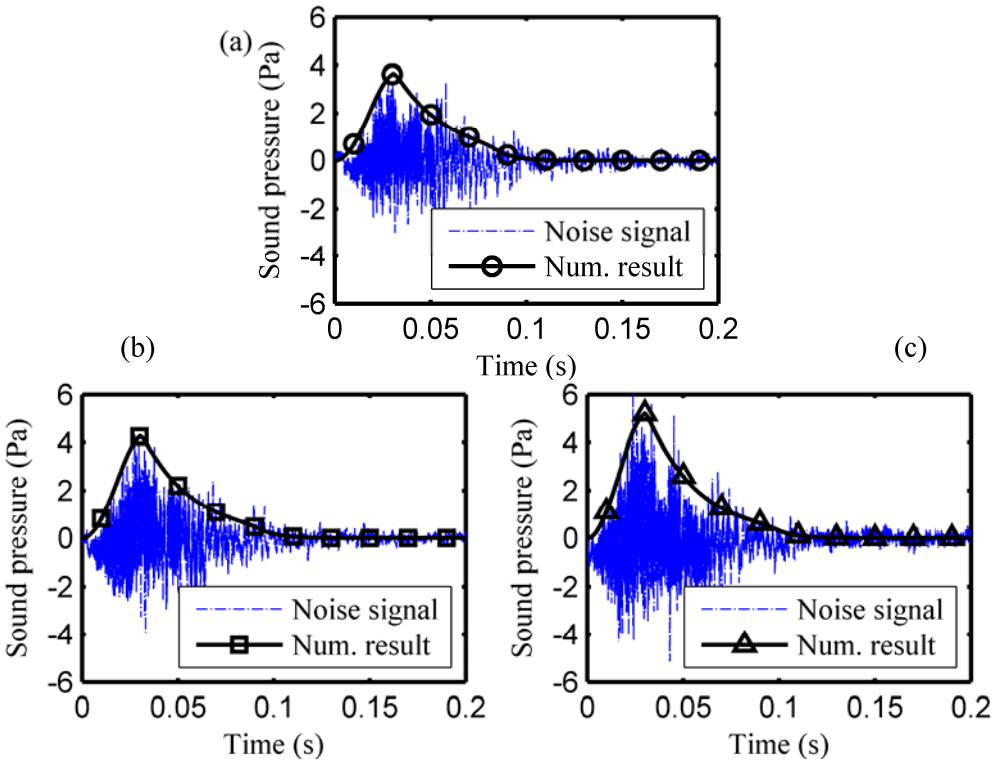

Figure 5-9 Prediction of the radiated exhaust noise in time-domain.

The initial pressures are, respectively, (a) 0.36 MPa, (b) 0.40 MPa and (c) 0.48 MPa.

5.3.2 Noise spectrum prediction

According to the approximation of piston acoustic source, the SPL is calculated and compared with the measured results at the initial cylinder pressures of 0.40 MPa and 0.48 MPa, as shown in Figures 5-10 and 5-11. Due to the effect of the equivalent factor $2k^2d_e^2$ of quadrupoles, the monopole sources play a major role in contributing to the low-frequency of sound pressure, whereas the quadrupoles primarily contribute to the high-frequency. The predicted SPL accords with the experiments well, even though the details are not exactly identical, especially at the low-frequency. This can be explained by the filtering effect of the Bessel function. On the other hand, the reason is also that the far-field condition becomes not suitable for the calculation model of sound radiation with longer wavelength. Nevertheless, the mean absolute error of octave band SPL is less than 1.5

dB, and the maximum difference is only 2.7 dB at the center frequency 8 kHz as shown in Figure 5-11. Therefore, the presented SPL prediction of transient exhaust through the sintered bronze silencer in frequency-domain is reasonable.

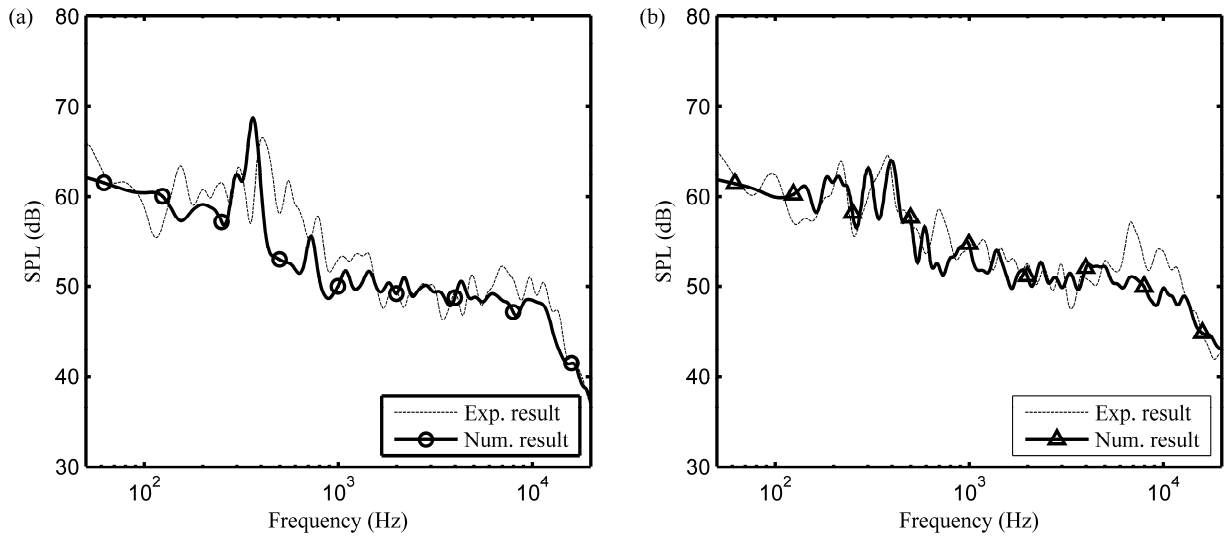

Figure 5-10 SPL prediction of the radiated exhaust noise.

The initial pressures are, respectively, (a) 0.40 MPa and (c) 0.48 MPa.

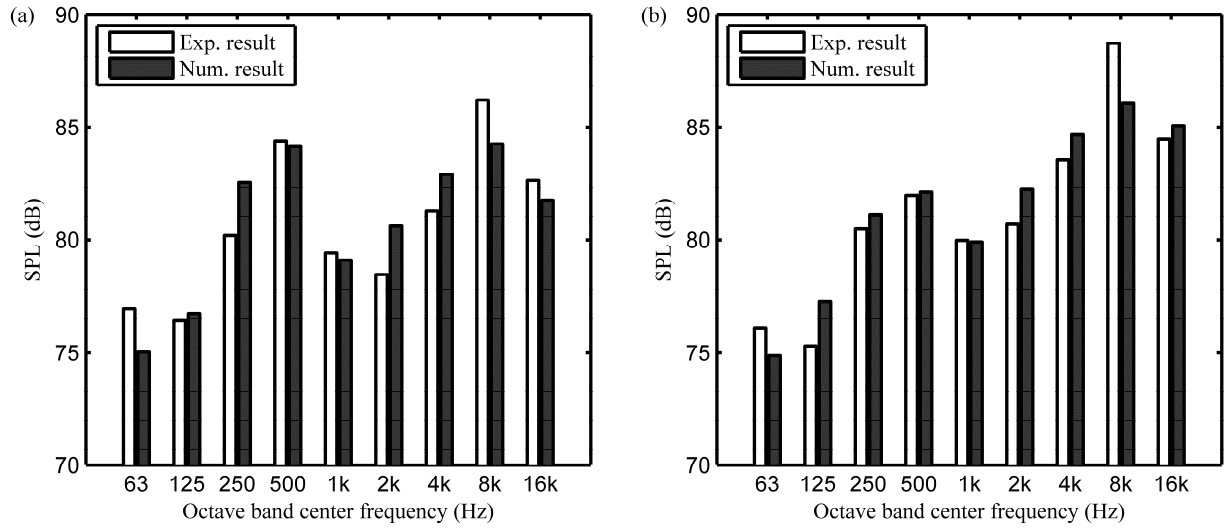

Figure 5-11 Octave band SPL prediction of the radiated exhaust noise.

The initial pressures are, respectively, (a) 0.40 MPa and (c) 0.48 MPa.

The above discussions show that the radiated exhaust noise can be predicted both in the time-domain and frequency-domain by using the presented mathematic models. The impulse fluctuation of exhaust noise is related to the transient mass flow. The piston acoustic source approximation can be used to analyze the SPL spectrum at a far-field observation point. Such researches will provide references for the study of impulse exhaust and its radiated noise and also for the study of suppression strategies.

5.4 Results of impulse exhaust noise suppression

Because the amplitude of impulse exhaust noise is related to the mass flow rate at the outlet of exhaust system as the previous discussions, the noise is suppressed by smooth the mass flow rate according to the semi-active control strategy by controlling the opening process of pneumatic valve. The verify experiments were carried out based on the introduced simplified cylinder exhaust test-bed with a modified 3/2-way directional valve. Then the results of such strategy will be presented in details.

5.4.1 Exhaust with normal solenoid valve

Firstly, the results of exhaust with an normal solenoid valve are presented as references. The structure of solenoid valve is same as the modified valve shown in Figure 5-2, but driven by a pilot solenoid valve. The valve can complete the reversing operation in a very short time due to the small displacement of poppet valve. However, since the intake and exhaust of pilot valve take a time, the response of switch is about 50 ms. Figure 5-12 shows experimental results of the cylinder pressure and its derivative with different initial pressures 0.33 MPa, 0.38 MPa and 0.44 MPa. The valve was

opened to discharge the cylinder air at the time 0.2 s in every exhaust process for synchronism. As previously mentioned, the pressure decreases as an approximate power function after the delay time of the valve response. The curves are smoother than that of exhaust in PFC/B system due to the fixed cylinder volume. The pressure derivative reaches the maximum value at the very beginning of the exhaust process, and then decreases gradually. The total exhaust times are about 500 ms, 540 ms and 570 ms, respectively, if considering the response time. Additionally, the higher initial pressure means there are more gases and more potential energy inside the cylinder. Thus, it will generate much more impact and takes a longer time.

Figure 5-13 shows the results of the recorded noise signals and the calculated mass flow rate of valve throat. There are some small noise signals appearing before the noises reaching to the peak value, which represents the noise generated by the exhaust of pilot solenoid valve. The peak SPL are 136.7 dB(A), 137.8 dB(A) and 139.2 dB(A), respectively, as references.

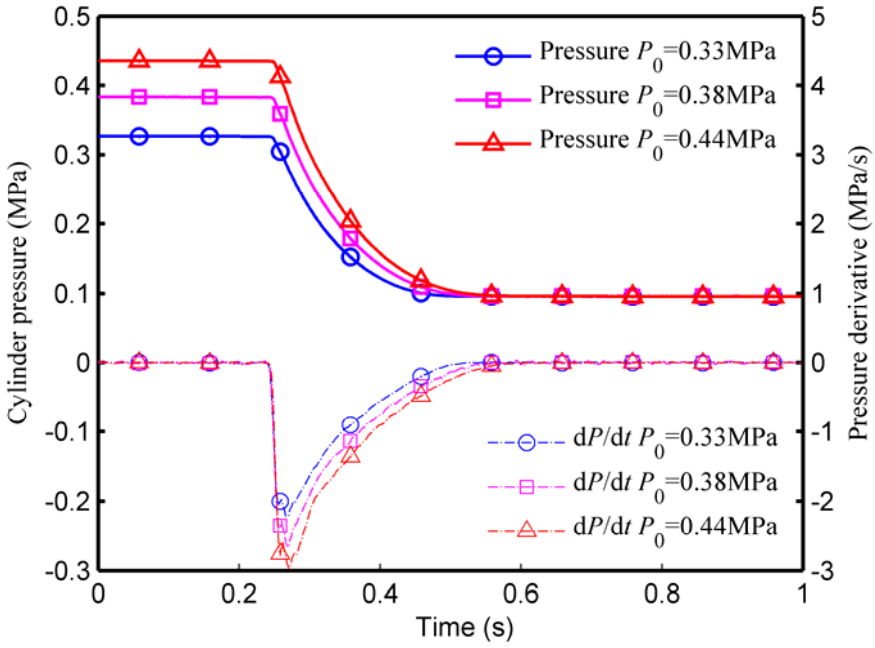

Figure 5-12 The cylinder pressure and its derivative of exhaust with an original solenoid valve.

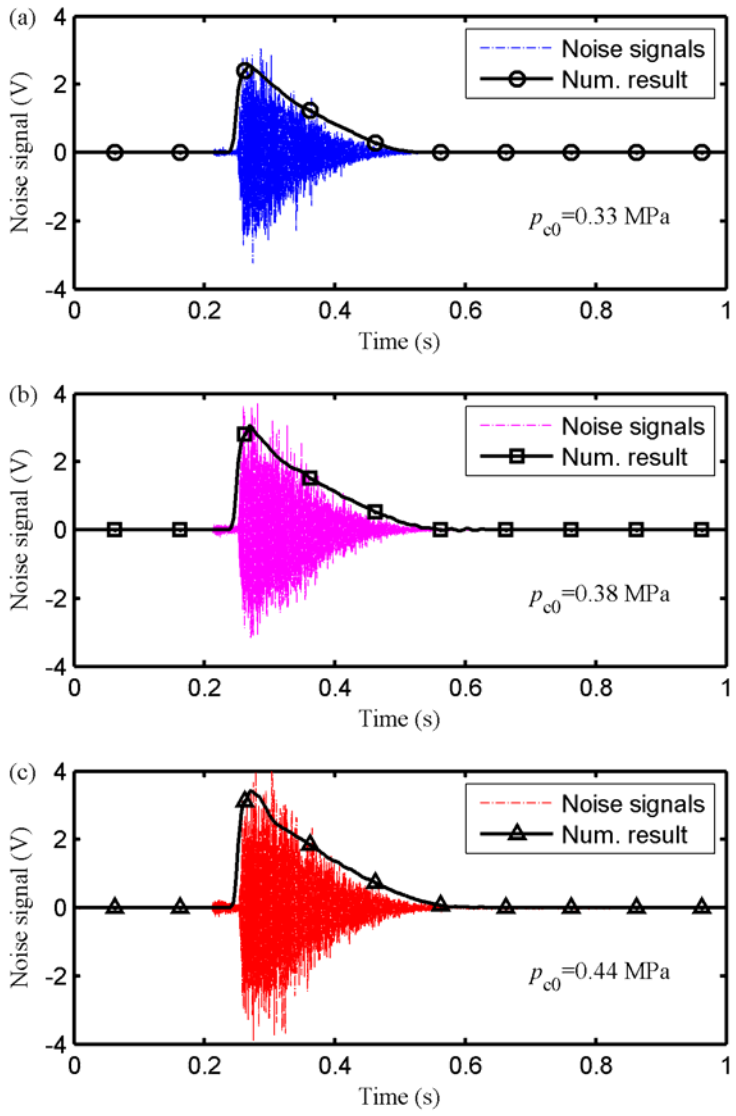

Figure 5-13 The noise signals and mass flow rate at the valve throat of exhaust with an original solenoid valve.

5.4.2 Exhaust with modified valve

In accordance with the strategy of noise suppression, the expected exhaust time are setting as 300 ms, 400 ms and 500 ms, which are identified by slow, medium and fast. The expected pressure can be solved by Equation (4-7) and then the effective cross-sectional area of valve can be obtained by Equation (4-5). Controlling the servo motor rotates according to the designed speed, the poppet valve of modified pneumatic valve will be moved as an expected specific curve as shown in Figure

5-14. The area changing curves in Figure 5-14 were according to the expected movements with initial pressure 0.44 MPa and recorded by the encoder signals. Such curves in Figure 5-14 show that the poppet valve was controlled to open a small area at 0.2 s suddenly, and then was droved to increase the area nonlinearly until to the limit position. The area has a maximum value 5.25×10^{-4} m^2 because of the structure limit of valve. The area changing of exhaust with other two initial pressures 0.33 MPa and 0.38 MPa are similar, but have some minor differences such as the step area values at the beginning.

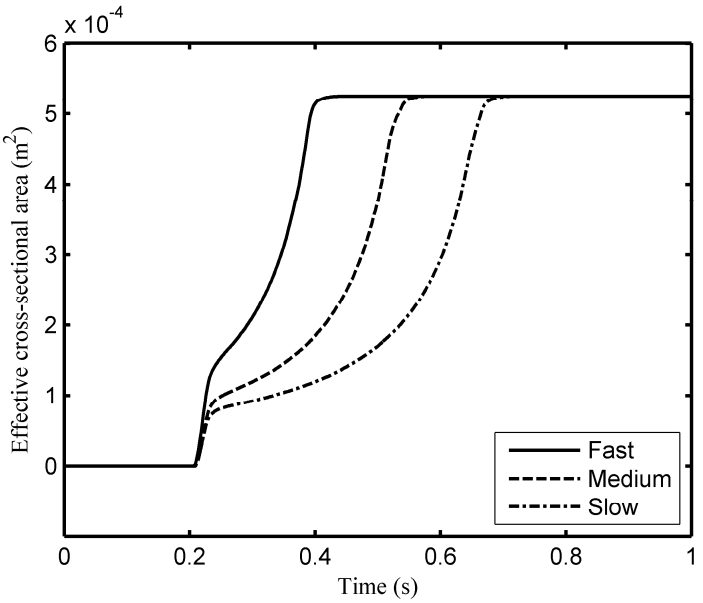

Figure 5-14 The effective cross-sectional area of valve according to the different expected exhaust time.

Under control of the opening process of valve according to the designed curves, the exhaust process will carry out in accordance with the expectations. The cylinder pressure curves of exhaust with different designed area changing are shown in Figure 5-15. The initial cylinder pressures are 0.33 MPa, 0.38 MPa and 0.44 MPa, respectively. It can be seen that the pressure changes are significantly different from that controlled by a solenoid valve as shown in Figure 5-12. The pressure decreases as an approximate straight line drawn by dash curves, of which the gradient is

related to the initial pressure and the expected exhaust time. In addition, the delay is shorter than that in the exhaust controlled by a solenoid valve due to the rapid response of motor rather than the pilot valve. The pressure decreases nonlinearly in the later exhaust process, because of the limit of effective cross-sectional area of valve and the complex phenomenon during the subsonic exhaust.

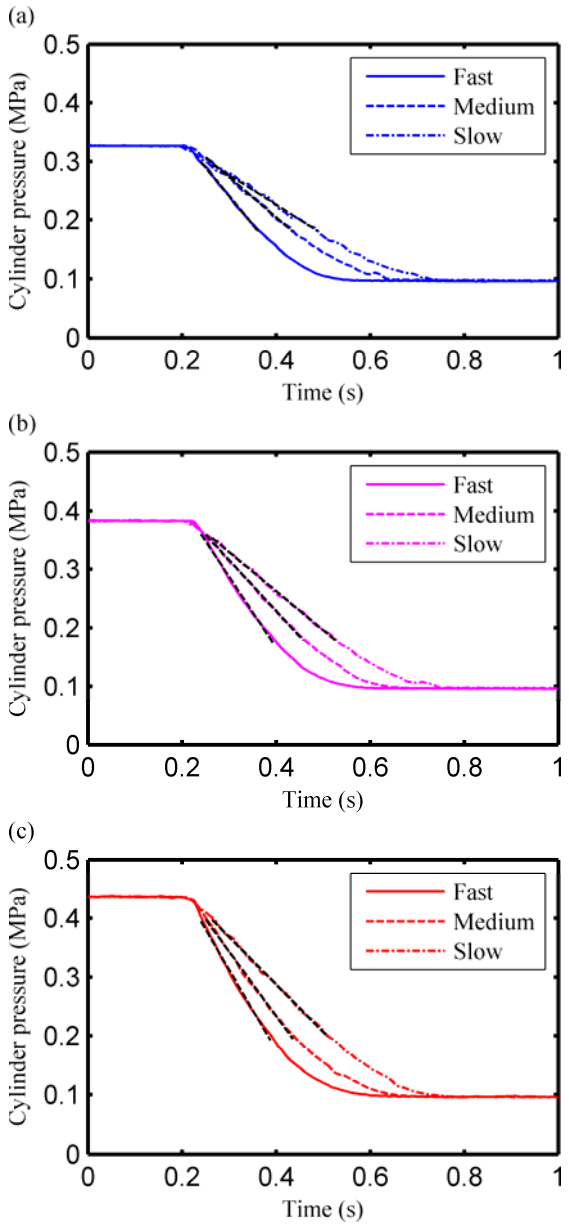

Figure 5-15 The cylinder pressures according to the fast medium and slow opening process of valve with different initial pressures, (a) 0.33 MPa; (b) 0.38 MPa; (c) 0.44 MPa.

Figure 5-16 shows the suppressed impulse exhaust noise based on the three groups of valve opening processes and the calculated mass flow rate of the flow through valve. The envelope of such noise signals are very different from the noise generated by the exhaust with a solenoid valve. There are no small noises at the beginning, which exist in the solenoid valve exhaust causing by the pilot valve exhaust. The noise signals reach the peak values and stay for a certain time approximately, as the same as the expected effect. Apparently, the slower opening process of valve extends the exhaust process, thus the energy of noise is dispersed. Compared to the exhaust with a solenoid valve, the peak SPL of exhaust with the presented control strategy is reduced obviously.

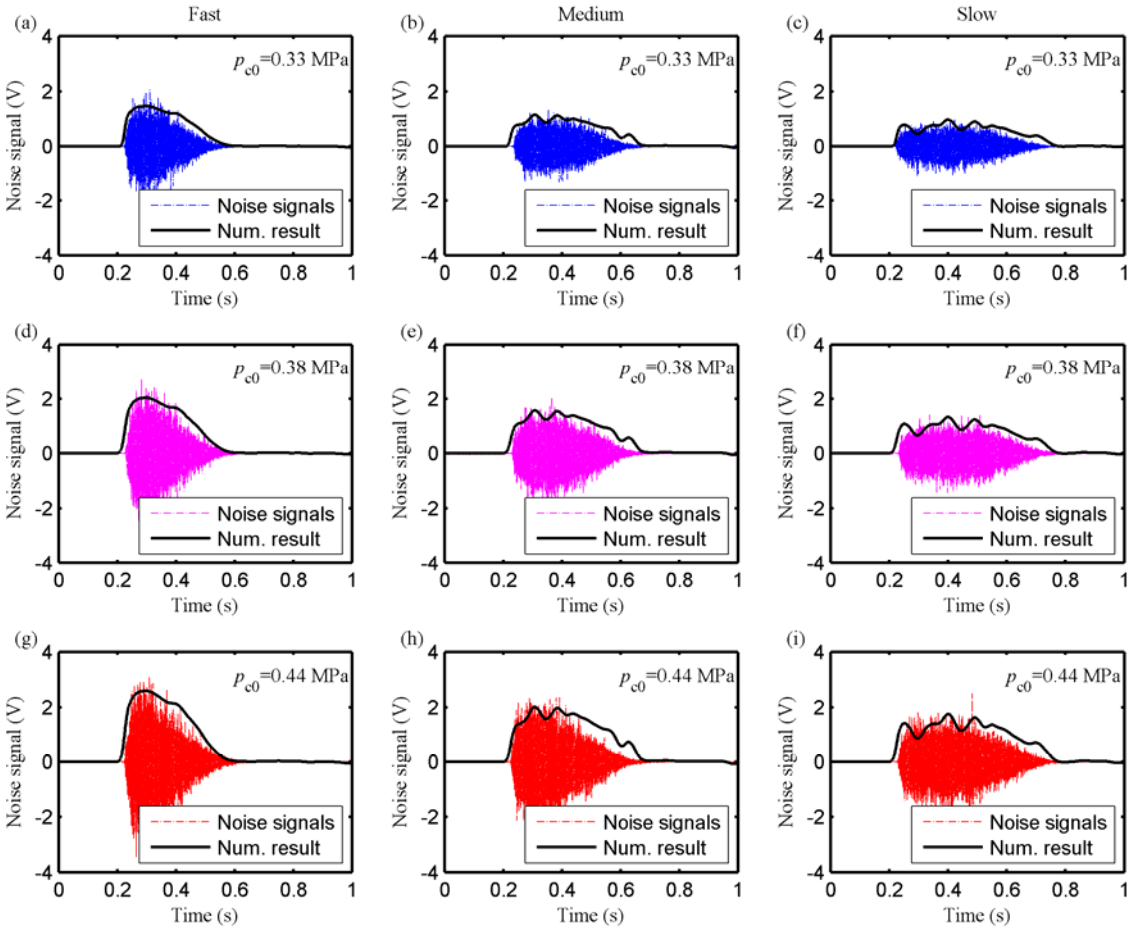

Figure 5-16 The noise signals and mass flow rate at the valve throat of exhaust according to the fast medium and slow opening process of valve with different initial pressures, (a) 0.33 MPa; (b) 0.38 MPa; (c) 0.44 MPa.

5.4.3 Discussions of noise suppression

The above experimental results show intuitively that both the pressure and exhaust noise were changed significantly due to the semi-active noise control strategy by controlling the valve opening process. The pressure decreasing linearly means the mass flow rate is relatively stable especially during the sonic exhaust stage, reflected by the stable peak value of noise. Then some discussions are presented to checkout the effect of the semi-active noise control strategy by comparing the parameters and the noise criterions of the experimental results.

1) Exhaust extended ratio

Exhaust extended ratio is the ratio of the extended exhaust time and the exhaust time with normal solenoid valve. It is used to evaluate the aerodynamic performance of the impulse exhaust, which is shown in Figure 5-17. It can be seen that the extended ratio almost between 20 percents to 55 percents increases if the longer expected exhaust time is chosen. In fact, the exhaust extended time is almost same when the cylinder air discharges with different initial pressures, but the ratio is smaller while there is higher pressure air in the cylinder before exhaust.

2) Noise reduction of peak SPL

The noise reduction of peak SPL is one of the most concerned criterions of the impulse exhaust noise suppression. Figure 5-18 shows the results of the noise reductions of peak SPL. The maximum noise reductions of peak SPL are 9.4 dB(A), 8.3 dB(A) and 4.7 dB(A), respectively, with different initial cylinder pressures when the valve is opened as the slow curves. By the strategy of noise control, the peak SPL is reduced at least about 2 dB(A), which means the sound energy at the peak is suppressed about 36 percents. In addition, it can be seen that there is a better effect of suppression in the low-pressure gas discharging.

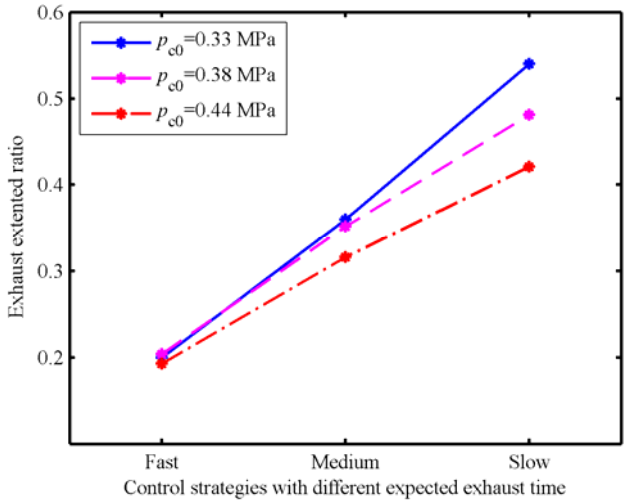

Figure 5-17 Exhaust extended ratio.

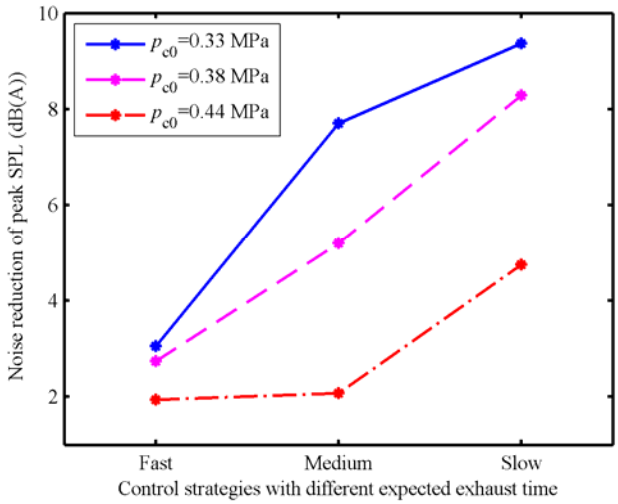

Figure 5-18 Noise reduction of peak SPL.

3) Sound exposure level

Comparing the sound exposure level shown in Figure 5-19, as defined by Equation (4-3) or (4-4), the results are similar with the peak SPL reduction. With the semi-active control strategy, the sound exposure level is reduced. The exposure energy of impulse noise is suppressed at least 7 percents when the initial pressure is 0.44 MPa and the exhaust controlled with the fast open curve of the valve area.

4) Duration time of impulse noise

The presented strategy is to limit the peak SPL of impulse exhaust noise by smoothing the amplitude of noise. Thus, the duration time of impulse noise will be extended as shown in Figure 5-20. The most longer duration time in this study is about 2.5 times than that of reference exhaust. From the point of view that the noise threshold increases 3 dB if the exposure time decreases by half, the presented strategy has an acceptable effect on the suppression of impulse exhaust noise.

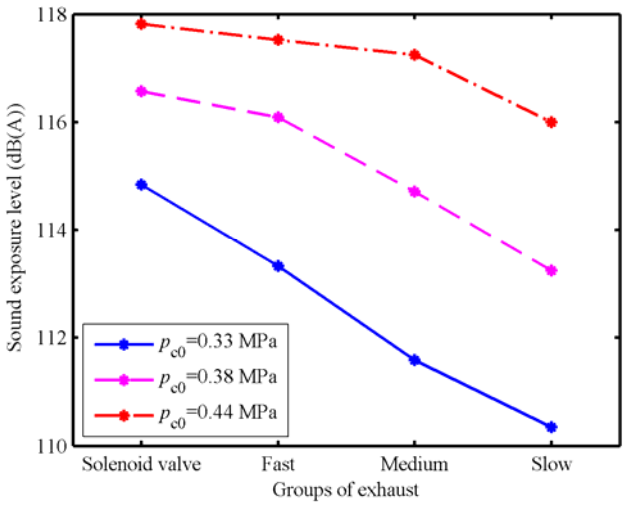

Figure 5-19 Sound exposure level.

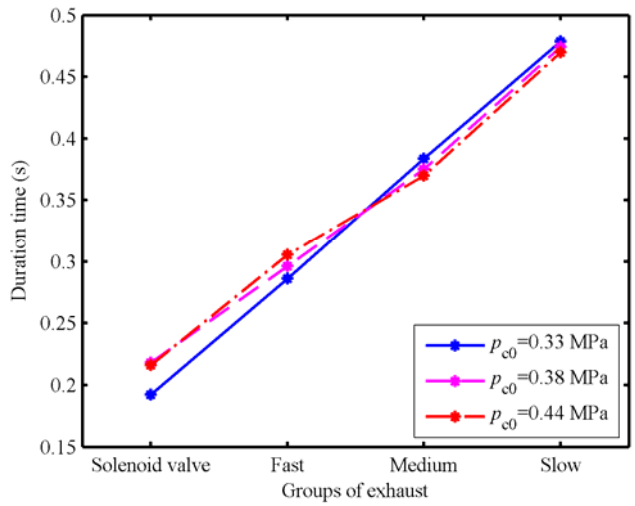

Figure 5-20 Duration time of impulse noise.

5) Octave band SPL

Additionally, the spectral characteristics of impulse exhaust noises with and without controlling are shown in Figure 5-21. It can be seen from the octave spectrum that the control strategy has a significant suppression of impulse exhaust noise (about 10 to 20 dB reduction) in the frequencies below 250 Hz, where the noise source is mainly caused by the shock of mass flow. In the high-frequency, the strategy of changing the valve opening process is not obvious but still has a small effect in the attenuation.

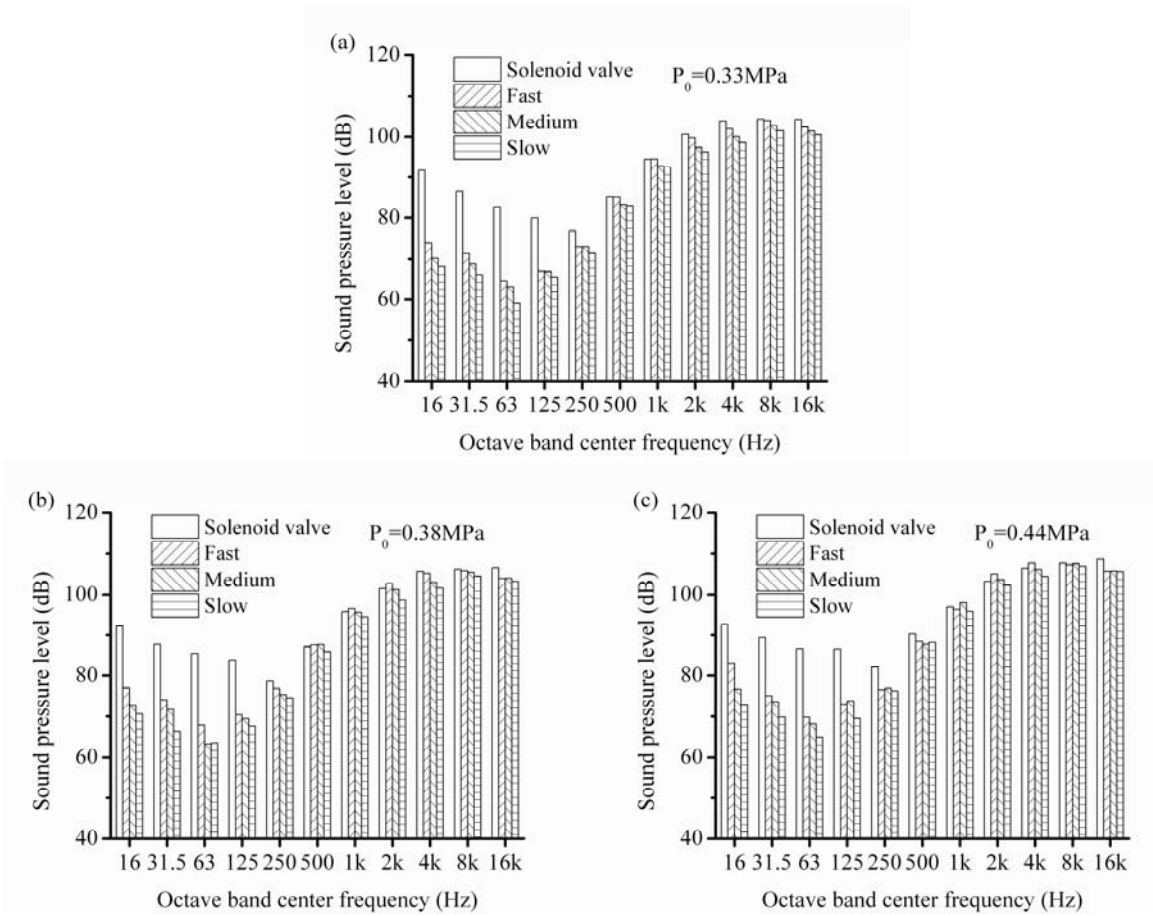

Figure 5-21 Octave band SPL of noise generated by the impulse exhaust.

Overall, during the impulse exhaust process with same initial cylinder pressure or same initial potential energy, the energy is released and converted to kinetic energy in a short time. The impulse

exhaust noise is essentially generated in such an energy conversion process. Extending the exhaust disperses the impulse noise in the time-domain, so that the noise is diffused to a longer period of time and the peak valve is reduced. The presented strategy of controlling the valve opening process makes the reduction effect of the noise peak maximally, since the peak can be controlled at a stable value especially during the sonic exhaust stage. In the experiments, the suppressed impulse exhaust noises became to sound much quieter and acceptable. On the other hand, performance may be affected if the exhaust lasts too long especially in some pneumatic systems with special requirements. In the practical applications the common used silencers such as porous diffusion silencers also have this problem, that the exhaust extended rate may reach to 40% due to the resistance of sound absorption material especially when the amount of exhaust air is large. Nevertheless, some appropriate additional exhaust time is also accepted as long as the systems can work normally.

Chapter 6 Conclusions and future work

6.1 Main conclusions

As presented in previous chapters, characteristic analysis and suppression strategy of impulse exhaust noise have been investigated both theoretically and experimentally. The study was based on the impulse exhaust of pneumatic systems and paid attention to both the aerodynamic properties and the flow noise characteristics. Considering the relation between the exhaust flow and the radiated noise, a strategy of noise suppression was presented and verified by experiments. In this chapter, a brief summary of the whole research and major conclusions obtained in the study are given.

1. The aerodynamic properties of impulse exhaust based on typical pneumatic exhaust systems have been investigated. A simplified aerodynamic model with a dynamic equation of piston is derived from thermodynamics and presented to analyze the exhaust process. The aerodynamic model of porous material with rigid frame such as sintered bronze was established from the pressure drop described by the Ergun equation. According to the aerodynamic models, the flow parameters during the impulse exhaust were obtained and verified by experiments.
2. The sound sources of impulse exhaust noise were studied based on the Lighthill's general theory of aerodynamic noise. This mass flow rate is related to the monopole source of impulsive exhaust noise. With piston acoustic source approximation of sintered bronze silencer, the sound pressure of radiated noise at far field observation point have been predicted by the flow parameters calculated from the simplified aerodynamic model.

3. A semi-active noise control strategy have been presented to suppress the impulse exhaust noise especially to reduce the peak SPL. The principle was introduced that is to smooth the impulse noise by the linearization of cylinder pressure decreasing and the mass flow rate at the valve throat. Experiments show that the strategy can reduced both the peak SPL and sound exposure level obviously.

6.2 Future work

Although some work have been done on the aerodynamic properties of impulse exhaust, the sound sources and radiated noise characteristics of impulse noise, the investigation of noise suppression, much further work is required to investigate the mechanism and to improve the reduction of impulse exhaust noise in industry. The future work can be focused on the following aspects.

1. The aerodynamic model presented in this work is simplified based on the control volume, which ignores the complex structure of the real pneumatic system. The computational fluid dynamics (CFD) could be used to simulate the detailed impulse flow and also to predict the radiated noise by aerodynamic noise theories.
2. The introduced noise control strategy was verified by a modified valve with servo motor. In the future, a valve with simple structure to achieve the effective area control could be studied. Furthermore, combining the presented strategy with classical silencers could be investigated to improve the suppression effect.

References

1. David A. Bies and Colin H. Hansen, Engineering Noise Control-Theory and practice[M], Second edition, E & FN Spon, London, 1997.
2. H. D. Baumann and W. B. Coney, "Noise of gas flows", Chap. 15 in Noise and Vibration Control Engineering-Principles and Applications[M], Second edition, edited by Istvan L. Ver and Leo L. Beranek, Wiley, New York, 2006.
3. D. M. Jang, Gas Flow in Internal Combustion Engine[M], Beijing: China Machine Press, 1985. (in Chinese)
4. Miller GT. Living in the Environment-principles, connections and solutions[M]. Belmont: Brooks/Cole Publishing Company, 2000.
5. Miller GT. Environmental Science-Working with the Earth[M]. Belmont: Brooks/Cole Publishing Company, 2001.
6. D.Y. Maa, P.Z. Li, G.H. Dai, H.Y. Wang, Shock associated noise from choked jets[J], Acta Acustica, 3 (1980) 172-182. (in Chinese)
7. H.S. Shi, S.D. Zhao, Prediction of radiation characteristic of intermittent exhaust noise generated via pneumatic value[J], Noise Control Engineering Journal, 57 (2009) 157-168.
8. J. X. Li, S. D. Zhao and K. Ishihara, Study on acoustical properties of sintered bronze porous material for transient exhaust noise of pneumatic system[J], J Sound Vibr., 332(11), (2013),2721-2734.
9. S.D. Zhao, J. Wang, J. Wang, Y. He, Expansion-chamber muffler for impulse noise of pneumatic frictional clutch and brake in mechanical presses[J], Applied Acoustics, 67 (2006) 580-594.
10. J.A. Daggerhart, E. Berger, An evaluation of mufflers to reduce punch press air exhaust noise[J], Noise Control Engineering, 4 (1975) 120-123.
11. S. Sahlin, Origins of punch press and air nozzle noise[J], Noise Control Engineering, 3 (1974) 4-9.
12. J. X. Li, K. Ishihara and S. D. Zhao, Experimental study on performance of various mufflers for intermittent exhaust noise reduction[C], Inter-Noise2011, (2011).
13. S. Zimmermann and R. Ellis. Engineering Acoustics: An Introduction to Noise Control[M], Second Edition. London, UK, Springer, 2009.
14. Rosenblith, W. A. and Stevens, K. N. Noise and man.. Handbook of Acoustic Noise Control[M] , WADC TR52-204, Vol. 2. 1953
15. Dejong, R. G. and Groeneveld, Y. CEC joint project on impulse noise: Overall results of the field survey[C]. In Proc . of Inter-Noise. (1985), 905-908.
16. Flindell, I. H. and Rice, C. G. CEC joint project on annoyance due to impulse noise: Laboratory studies. ISVR Memo 677, (1986), 1984-1985.
17. International Organisation for Standardization Draft Addendum ISO 3891/DAD 1, Acoustics, (1981).
18. IEC-Pub. 179A Precision sound level meters additional characteristics for the measurement of impulsive sounds, (1973).
19. S. Raghunathan, H. D. Kim and T. Setoguchi, Impulse noise and its control[J], Prog. Aerospace Sci., 34, (1998)
20. Morata TC, Themann CL, Randolph RF, et al. Working in noise with a hearing loss perceptions from workers,supervisors,and hearing conservation program managers[J]. Ear Hear, 2005, 26 (6): 529-545.
21. M.J. Lighthill, On sound generated aerodynamically: Part 1[J]. General theory, Proceedings of the Royal

Society of London A, 211 (1952) 564-587.
22. M.J. Lighthill, On sound generated aerodynamically: Part 2[J]. Turbulence as a source of sound, Proceedings of the Royal Society of London A, 214 (1954) 1-32.
23. Lighthill MJ. The Bakerian Lecture, 1961. Sound Generated Aerodynamically[J]. Proceedings of the Royal Society of London Series A, Mathematical and Physical Sciences, 1962, 267 (1329): 147-182.
24. Kobrynski M. General Method for Calculating the Sound Pressure Field Emitted by Stationary and Moving Jets[J]. AFOSR-UTIAS Symposium on Aerodynamic Noise,Toronto, 1968: 112-130.
25. Goldstein M, E. Aeroacoustics[M]. McGraw: Hill Book Company, 1964.
26. Ribner HS. The Generation of Sound by Turbulent Jets-Advances in Applied Mechanics[M]: Academis Press, 1964.
27. Doak PE. A Critical Review of Conceptional Adequacy and Physical Scope of Existing Theories of Aerodynamic Noise[J]. Journal of Sound and Vibration, 1972, 25: 263-335.
28. Dowling AP, Ffowcs Williams JE, Goldstein ME. Sound Production in a Moving Stream[J]. Phil Trans, roy, Soc(London), 1978, 288: 321-349.
29. Ffowcs Williams JE. Jet Noise at very Low and very High Speed[J]. AFOSR-UTIAS Symposium on Aerodynamic Noise,Toronto, 1968: 131-146.
30. Powell A. On the Mechanics of Choked Jet Noise[J]. ProcPhysSoc, 1953, 66: 313-327.
31. S. Ergun, A.A. Orning, Fluid flow through packed columns[J], Chemical Engineering Progress, 48 (1952) 89-94.
32. I.F. Macdonald, M.S. El-Sayed, K. Mow, F.A.L. Dullien, Flow through porous media-the Ergun equation revisited[J], Industrial & Engineering Chemistry Fundamentals, 18 (1979) 199-208.
33. J.L. Lage, B.V. Antohe, Darcy's experiments and the deviation to nonlinear flow regime[J], Journal of Fluids Engineering, 122 (2000) 619-625.
34. N. Robert K, Physical insight into the Ergun and Wen & Yu equations for fluid flow in packed and fluidised beds[J], Chemical Engineering Science, 57 (2002) 527-534.
35. M. Mayerhofer, J. Govaerts, N. Parmentier, H. Jeanmart, L. Helsen, Experimental investigation of pressure drop in packed beds of irregular shaped wood particles[J], Powder Technology, 205 (2011) 30-35.
36. J.-F. Allard, N. Atalla, Propagation of sound in porous media: modeling sound absorbing materials[M], Second edition, Wiley, New York, 2009.
37. D.L. Johnson, J. Koplik, R. Dashen, Theory of dynamic permeability and tortuosity in fluid-saturated porous media[J], Journal of Fluid Mechanics, 176 (1987) 379-402.
38. S.R. Pride, F.D. Morgan, A.F. Gangi, Drag forces of porous-medium acoustics [J], Physical Review B, 47 (1993) 4964-4978.
39. Y. Champoux, J.-F. Allard, Dynamic tortuosity and bulk modulus in air-saturated porous media[J], Journal of Applied Physics, 70 (1991) 1975.
40. D. Lafarge, Dynamic compressibility of air in porous structures at audible frequencies[J], The Journal of the Acoustical Society of America, 102 (1997) 1995-2006.
41. M. Fringuellino, C. Guglielmone, Progressive Impedance Method for the classical analysis of acoustic transmission loss in multilayered walls[J]. Applied Acoustics, 59 (2000) 275-285.
42. A.K. Vashishth, P. Khurana, Waves in stratified anisotropic poroelastic media: a transfer matrix approach[J], Journal of Sound and Vibration, 277 (2004) 239-275.
43. C.M. Lee, Y. Xu, A modified transfer matrix method for prediction of transmission loss of multilayer acoustic materials[J], Journal of Sound and Vibration, 326 (2009) 290-301.
44. A. Hocine, B. Desmet and S. Guenoun, Numerical study of the influence of diesel post injection and exhaust gas expansion on the thermal cycle of an automobile engine[J], Appl. Them. Eng., 30, (2010) 1889-1895.

45. S. D. Morris, Choked gas flow through pipeline restrictions: an explicit formula for the inlet Mach number[J], Journal of Hazardous Materials, 50, 71-77, (1996).
46. F. Payri, A. Broatch, J.M. Salavert, D. Moreno, Acoustic response of fibrous absorbent materials to impulsive transient excitations[J], Journal of Sound and Vibration, 329 (2010) 880-892.
47. Bugaru M, Vasile O. Transfer matrix method for a single-chamber mufflers[J]. Proceedings of the 11th WSEAS International Conference on Applied Mathematics (MATH '07), 2007: 47-50.
48. Munjal ML. Velocity ratio-cum-transfer matrix method for the evaluation of a muffler with mean flow[J]. Journal of Sound and Vibration, 1975, 39: 105-119.
49. Munjal ML. acoustics of Ducts and Mufflers-With Application to Exhaust and Ventilation System Design[M]. Canada: John Wiley & Sons,Inc., 1987.
50. Cuesta M, Cobo P. Active control of the exhaust noise radiated by an enclosed generator[J]. Applied Acoustics, 2000, 61 (1): 83-94.
51. Cuesta M, Cobo P. Optimisation of an active control system to reduce the exhaust noise radiated by a small generator[J]. Applied Acoustics, 2001, 62 (5): 513-526.
52. Sathyanarayana Y, Munjal ML. A hybrid approach for aeroacoustic analysis of the engine exhaust system[J]. Applied Acoustics, 2000, 60 (4): 425-450.
53. Torregrosa AJ, Broatch A, Fernandez T, et al. Description and measurement of the acoustic characteristics of two-tailpipe mufflers[J]. Journal of the Acoustical Society of America, 2006, 119 (2): 723-728.
54. Ikeda T, Nishimura T, Ando T, et al. Resonance of elliptical perforated tube muffler[J]. Electronics and Communications in Japan Part Iii-Fundamental Electronic Science, 2000, 83 (8): 51-60.
55. Broatch A, Serrano JR, Arnau FJ, et al. Time-domain computation of muffler frequency response: Comparison of different numerical schemes[J]. Journal of Sound and Vibration, 2007, 305 (1-2): 333-347.
56. Sinder DJ. Speech Synthesis Using An Aeroacoustic Fricative Model[D]. New Brunswick Rutgers: The State of University of New Jersey, 1999.
57. E-P HYREG, Series VY1700. 14-10. www.smc.com
58. Zhao SD, Shang CY, Zhao ZG, et al. Radiation Characteristics of Intermittence Exhaust Noise[J]. Chinese Journal of Acoustics, 2000, 19 (4): 309-316.
59. Kinsler LE, Austin R. Frey, Alan B. Coppens, et al. Fundamentals of Acoustics[M]. New York: John Wiley & Sons, Inc., 2000.
60. Jeyapalan RK, Halliwell NA. Machinery Noise Predictions at the Design Stage Using Acoustic Modeling[J]. Applied Acoustics, 1981, 14 (5): 361-376.
61. Rabiner LR, Schafer RW. Digital Processing of Speech Signals[M]. New York: Prentice Hall, Inc., Englewood Cliffs, N. J. , 1978.
62. Webster AG. Acoustical Impedance, and the Theory of Horns and of Phonograph[J]. Proceedings of the National Academy of Sciences, 1919, 5 (7): 275-282.
63. Shi HS, Zhao SD. Pre-Reducing the Intermittent Exhaust Noise by Optimizing the Exhaust Pipeline at the Design Stage[J]. Imece 2008: Proceedings of the Asme International Mechanical Engineering Congress and Exposition, Vol 5, 2009: 61-66.
64. Shi HS, Zhao SD, Wen JP. An Improved Particle Swarm Optimization for Pre-denoise at the Exhaust Pipeline Design Stage[J]. Ieem: 2008 International Conference on Industrial Engineering and Engineering Management, Vols 1-3, 2008: 780-784.
65. V.B.PANICKER, M.L.MUNJAL. Aeroacoustic analysis of straight-through mufflers with simple and extended tube expansion chambers[J]. Journal of the Indian Institute of Science, 1981, A (63): 1-19.
66. Jun W, Sheng-dun Z, Hu-shan S, et al. Method to calculate and counterbalance the inertia forces of slider-crank mechanisms in high-speed presses[J]. Academic Journal of Xi'an Jiaotong University, 2009, 21 (3): 141-148.

67. P.M. Morse, K.U. Ingard, Theoretical acoustics[M], McGraw-Hill, New York, 1968.
68. Sintered Type Quletalre Mufflers, Compressed Air Mufflers, Section 8, FIT-8-6. www.norgren.com.
69. L.P. Feng, D.Y. Maa, Relations between pulsed jet noise and steady jet noise[J], Acta Acustica, 15 (1990) 378-383. (in Chinese)
70. L.E. Kinsler, A.R. Frey, A.B. Coppens, J.V. Sanders, Fundamentals of acoustics[M], Fourth edition, Wiley, New York, 1982.
71. N. Curle, The influence of solid boundaries upon aerodynamic sound[J], Proceedings of the Royal Society of London. Series A. Mathematical and Physical Sciences, 231 (1955) 505-514.
72. D.A. Russell, J.P. Titlow, Y. Bemmen, Acoustic monopoles, dipoles, and quadrupoles: an experiment revisited[J], American Journal of Physics, 67 (1999) 660-664.
73. B. Lagrain, L. Boeckx, E. Wilderjans, J.A. Delcour, W. Lauriks, Non-contact ultrasound characterization of bread crumb: Application of the Biot–Allard model[J], Food Research International, 39 (2006) 1067-1075.
74. M. Villot, C. Guigou, L. Gagliardini, Predicting the acoustical radiation of finite size multi-layered structures by applying spatial windowing on infinite structures[J], Journal of Sound and Vibration, 245 (2001) 433-455.

Acknowledgement

During the past years of my Ph.D study, I was lucky to receive a lot of help and cooperate with such excellent colleagues. Here, I would like to thank all of the people who have supported me and helped me. I would also like to thanks the people who are the most important in my life.

First of all, I have a sincere desire to say “Thank you” to my supervisors Prof. Dr. Kunihiko Ishihara and Prof. Dr. Junichi Hino from the University of Tokushima and Prof. Dr. Shengdun Zhao from Xi’an Jiaotong University. Aside from the support in research, I also got very important suggestion about my outlook on life. Without their support, encouragement, and guidance, I would not get my achievements today.

Secondly, I would like to thank the Double Degree Program between the University of Tokushima and Xi’an Jiaotong University. It provides a good chance for me to study abroad and offers a financial support for my study.

Thirdly, I would like to thank Dr. Hushan Shi for his guidance in experiment and helpful suggestion in writing papers. Thanks Mr. Junhang Guo, Mr. Bo Wu for studying and living in Japan together and also their assistance in research. Thanks Kohno Sensei for Japanese teaching and many helps for my living in Japan. Thanks all the members in CICEE, Dr. Pankaj Koinka, Dr. Walter Carpenter, Dr. Pangpang Wang, Dr. Dongyan Zhang and Asada San.

Then, I would like to thank all the members in the research group, Dr. Tsuji, Ms. Shuqin Fan, Mr. Bin Zhong, Mr. Jintao Liang, Mr. Renfeng Zhao, and also all of the friends in Japan.

Finally, on a more personal note, I wish to express my deepest appreciation to my family for their support, encouragement and love. Especially, thanks my wife for her love and accompanying.

Publications

Journals

1. Jingxiang Li, Shengdun Zhao, Kunihiko Ishihara, "Study on acoustical properties of sintered bronze porous material for transient exhaust noise of pneumatic system", Journal of Sound and Vibration, Vol. 332, Page 2721-2734, May, 2013.

2. Jingxiang Li, Shengdun Zhao, Kunihiko Ishihara, Hushan Shi, "Numerical and experimental studies on aerodynamic characteristics of pneumatic exhaust with perforated panel muffler", Advanced Materials Research, Vol. 291-294, Page 2125-2129, July, 2011.

International Conferences

1. Jingxiang Li, Kunihiko Ishihara, Shengdun Zhao, “Study on Transient Exhaust Process of Pneumatic System with Sintered Bronze Silencer: Modeling and Experimental Verification”, the 6th International Conference on Advanced Materials Development and Performance (AMDP 2011), Tokushima, Japan, Jul. 2011.(Oral)

2. Jingxiang Li, Shengdun Zhao, Kunihiko Ishihara, Hushan Shi, “Numerical and Experimental Studies on Aerodynamic Characteristics of Pneumatic Exhaust with Perforated Panel Muffler”, the International Conference on Advanced Engineering Materials and Technology (AMET 2011), Sanya, China, Jul. 2011. (Oral)

3. Jingxiang Li, Kunihiko Ishihara, Shengdun Zhao, “Experimental Study on Performance of Various Mufflers for Intermittent Exhaust Noise Reduction”, Proceedings of INTER-NOISE 2011,

the 40th International Congress and Exposition on Noise Control Engineering, Osaka, Japan, Sep. 2011. (Oral)

4. Jingxiang Li, Shengdun Zhao, Kunihiko Ishihara, " Insertion loss analysis of perforated panel muffler using finite element method with equivalent fluid model", The IEEE International Conference on Industrial Engineering and Engineering Management (IEEM 2012), Hongkong, China, Dec. 2012. (Poster)